

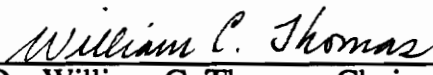
**Experimental Apparatus for Measuring Moisture Transfer in Porous Materials
Subject to Relative Humidity and Temperature Differences**

by

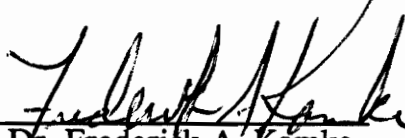
Robert Prentiss Crimm

Thesis submitted to the Faculty of the
Virginia Polytechnic Institute and State University
in partial fulfillment of the requirements for the degree of
Master of Science
in
Mechanical Engineering

APPROVED:



Dr. William C. Thomas, Chairman



Dr. Frederick A. Kamke



William H. Mashburn

April, 1992

Blacksburg, Virginia

LD

50445

V845

1992

C145

C.2

Experimental Apparatus for Measuring Moisture Transfer in Porous Materials Subject to Relative Humidity and Temperature Differences

by

**Robert Prentiss Crimm
Dr. William C. Thomas, Chairman
Mechanical Engineering**

(ABSTRACT)

A detailed design was developed of an apparatus to measure moisture transfer in porous materials. The apparatus is to be used to collect data to aid in the development of mathematical models which accurately describe this phenomena. The apparatus consists of dual environmental chambers between which a specimen material is sealed. The temperature of each chamber is controlled separately allowing nonisothermal test conditions. The relative humidity is maintained without the use of saturated salt solutions. The moisture transfer rate is measured by periodically weighing a desiccant column used to absorb moisture as result of diffusion across the specimen. The apparatus was built and used to verify a heat transfer model written to predict its thermal characteristics. The chamber temperature capabilities are 5°C to 60°C with up to a 20°C temperature difference across the specimen. The relative humidity limits are based on the heat transfer into or out of the system. High relative humidities (75 to 85 percent) are possible at chamber temperatures close to ambient, but decrease sharply at the extremely high or low temperatures and during nonisothermal operation. The apparatus maintains a constant temperature within $\pm 0.4^{\circ}\text{C}$ of the setpoint when subjected to varying

ambient temperatures. The spatial temperature variation close to the sample (within 25 mm) is within approximately $\pm 1^{\circ}\text{C}$ of the average chamber temperature. The relative humidity can be manually controlled to within $\pm .7$ percent RH. Automated control, complicated by a response lag, was within ± 1 percent RH.

Acknowledgements

I would like to thank Dr. W.C. Thomas for his continuous advice and support throughout this project. I would also like to thank Professor W.H. Mashburn and Dr. Fred A. Kamke for serving on my graduate committee and for their assistance and advice.

I gratefully acknowledge the National Institute of Standards and Technology for their financial and equipment support.

I also thank my parents for the encouragement and financial support they have provided me with throughout my college education.

The gratitude I feel toward my wife, Andrea, cannot be adequately expressed in words. She believed in me when I had doubts, and refused to let me quit when times were difficult. I am also very thankful to my children, Ryan and Allison, for their patience when I could not spend the time with them that I would have liked.

Table of Contents

I. Introduction	1
1.1 Background and Literature Review	1
1.2 Test Methods	4
1.2.1 ASTM Standard Test	5
1.2.2 Other Methods	8
1.2.3 Shortcomings of the Test Methods	12
1.3 Objectives of the Research	12
1.4 Target Operating Limits	12
II. Apparatus	13
2.1 Overview	13
2.2 Operation	15
2.3 Design	16
2.3.1 Modelling the Apparatus	16
2.4.2 Choice of Materials	19
2.4.3 The Chambers	20
2.4.4 The Desiccant and Bubble Columns	26
2.4.5 The Heat Exchangers and Resistance Heaters	32
2.4.6 The Sampling System	36
2.4.7 Pump system	36
III. Results	37
3.1 Isothermal Diffusion Simulation	37
3.2 Thermal Characteristics of the Chambers	37
3.2.1 Spatial Temperature Variations Within the Chamber	47
3.2.2 Time Varying Chamber Temperatures	47
3.3 Relative Humidity Control	51
3.4 Limits of Operation	53
3.4.1 Temperature limits	53
3.4.2 Relative Humidity Limits	53
3.4.2.1 Chamber Temperatures Lower Than Ambient Temperature	54
3.4.2.2 Chamber Temperatures Higher Than Ambient Temperature	57
3.5 Leak Tests	59
IV. Discussion and Recommendations	62
4.1 Increasing the Relative Humidity Operating Range	62
4.1.1 Chamber Temperatures Lower Than Ambient Temperature	62

4.1.1.1 Effect of Higher Recirculating Air Flow Rates ..	62
4.1.1.2 Effect of Decreasing the Chamber Size	64
4.1.1.3 Effects of Other Methods	64
4.1.1.4 Recommendations	68
4.1.1.5 Effect of the Heat Exchanger on the Operating Limits	68
4.1.2 Chamber Temperatures Higher Than Ambient Temperature	71
4.3 Relative Humidity Control	71
4.4 Pumps	73
4.5 Use of Acrylic	74
 V. Conclusions	 76
 References	 78
 Appendix 1	 79
 Appendix 2	 83
 Appendix 3	 91
 Vita	 94

List of Figures

Optimum relative humidity ranges for health	3
Typical ASTM 96-80 testing apparatus	6
Tveits (1966) moisture diffusion testing apparatus	9
Douglas's (1991) moisture diffusion testing apparatus	11
Overview of apparatus	14
Dimensions and construction details of the environmental chambers	21
Chamber inlets	23
Chamber outlet	24
Specimen holder	25
Thermocouple fittings	27
Bubble column	29
Desiccant column	30
Concentric pipe heat exchanger connections	34
Automated resistance heaters	35
Total moisture transfer vs time for a chamber with a diameter of 0.46 m.	39
Comparison of measured and calculated heat transfer for the isothermal case.	42
Measured heat transfer vs temperature difference across specimen	43

Calculated heat transfer vs temperature difference across specimen	44
Comparison of measured and calculated parasitic heat loss vs average chamber temperature	46
Spatial temperature variation testing procedure	48
Spatial temperature variation for a 13°C average chamber temperature and a 18°C temperature difference across the specimen	49
Spatial temperature variation for a 15°C chamber temperature and a 7°C temperature difference across the specimen	50
Time varying temperature fluctuations within the chamber	52
Relative humidity limits of the present apparatus when the chamber is operating at temperatures lower than ambient temperature	55
Relative humidity and temperature limits of present apparatus when the chamber is operating at temperatures higher than ambient temperature	58
Dynamic pump leak test setup	61
Differences in the operating limits for different flow rates vs temperature difference across the specimen	63
Differences in the operating limits for various chamber diameters vs temperature differences across the specimen	65
Differences in the operating limits for various insulation thicknesses vs temperature differences across the specimen	66
Total moisture transfer vs time for a chamber diameter of 0.305 m	67
Total moisture transfer vs time for a chamber diameter of 0.15 m	69

Operating limits with 0.3048 m chamber diameter, 0.0508 m chamber length, 1.7×10^{-3} m ³ /s flow rate, and 0.0762 m insulation thickness	70
Relative humidity limits when insulation is applied to the piping between the chamber and the pump for chamber temperatures higher than ambient temperature	72
Resistance network for mass diffusion through a specimen	80
Dewpoint temperature vs time for an air velocity of 0.037 m/s	85
Dewpoint temperature vs time for an air velocity of 0.11 m/s	86
Dewpoint temperature vs time for an air velocity of 0.22 m/s	87
Dewpoint temperature vs time for an air velocity of 0.44 m/s	88
Illustration of chamber thermal resistances	92

List of Tables

Results of the moisture diffusion simulation for white pine and gypsum	38
Mass of desiccant necessary to absorb 1 g of moisture for air with a 12°C dewpoint and a 22°C temperature	89

Nomenclature

a	-	Constant in Eq. 3
A	-	Area (m^2)
C_p	-	Constant Pressure Specific Heat (kJ/kg-K)
C_r	-	Heat Capacity Ratio C_{\min}/C_{\max}
D	-	Moisture Diffusion Coefficient (m^2/s)
D_{AB}	-	Vapor Mass Diffusion Coefficient (m^2/s)
g_d	-	Grams of Desiccant
g_w	-	Grams of Water
h	-	Convective Heat Transfer Coefficient ($W/m^2\text{-}^\circ C$)
h_m	-	Convective Mass Transfer Coefficient (m^2/s)
k	-	Thermal Conductivity ($W/m^\circ C$)
L	-	Length (m)
Le	-	Lewis Number
\dot{m}	-	Mass Flow Rate (kg/s)
\dot{m}''	-	Moisture Mass Flux ($kg/m^2\text{-}s$)
P	-	Pressure (Pa)
q	-	Heat Flux (W)
R	-	Ideal Gas Constant for Water Vapor (kJ/kg-K)
R	-	Mass Transfer Resistance ($m^2\text{-}s/kg$)
R	-	Thermal Resistance ($^\circ C/W$)

S	-	Shape Factor (m)
T	-	Temperature (°C)
U	-	Overall Heat Transfer Coefficient (W/m²-K)
x	-	Length (m)

Subscripts

1-4	-	Numbers used in Eq. 3 to indicate node locations. 2 and 3 are surface nodes. 1 and 4 are nodes in the air.
<i>a</i>	-	Air
a	-	Ambient
c	-	Chamber
c1	-	Chamber 1
c2	-	Chamber 2
d	-	Dry Material
f	-	Fluid
g	-	Saturated Water Vapor
i	-	Inlet
m	-	Mass
o	-	Outlet
<i>o</i>	-	Initial conditions
p	-	Pipe
spec	-	Specimen

S_n - Surface of the Specimen $n = 1, 2, \dots$

v - Vapor

w - Water

Superscripts

a - Constant in Eq. 2

Greek Symbols

γ - Moisture Content, Dry Basis (kg_w/kg_d)

ϕ - Relative Humidity

ρ - Mass Density

I. Introduction

The scope of this research project was to develop an alternative apparatus for measuring moisture diffusion in porous materials preparatory to data collection. The apparatus includes dual environmental chambers between which a material specimen is sealed. Air is externally conditioned for temperature and moisture content and then circulated through each chamber, thus providing the means to maintain relative humidity as well as temperature differences on opposite sides of the specimen.

1.1 Background and Literature Review

Prior to World War II, building construction in the United States was typically built with less concern for structural tightness, allowing air to freely move from the exterior to the interior and vice versa with little resistance. However, during the energy crisis of the World War II era, energy conservation became a major concern (Douglas, 1991). Buildings by necessity were more tightly built, better insulated, and sealed from air flow to make them more energy efficient.

The less energy conscious construction allowed air, and therefore air-borne moisture, to flow relatively freely into and out of buildings (Douglas, 1991). Though this was energy inefficient, it nevertheless prevented the danger of moisture buildup in the structural members and the walls. As construction was made tighter, air-borne moisture, driven by temperature and relative humidity differences between the inside and outside of the buildings, diffused through the building materials and accumulated inside the construction materials and insulation. This moisture buildup promoted the

unhealthy growth of molds and fungus, degradation of insulating properties of the insulation materials, and damage of the structural members through rot and frost (White, 1989).

In an effort to control moisture buildup in structures, research has been done which shows that vapor retarders in the form of polymer films placed in the wall will minimize moisture diffusion. These retarders, however, are difficult to apply properly and small holes can cause tremendous moisture penetration (Douglas 1991).

Sterling et al. (1985) points out that a moderate amount of moisture in air is actually beneficial. It has been shown that a relative humidity range between 40 and 60 percent in living environments is optimum for health and comfort. Very high or very low relative humidities, however, tend to promote the growth and spread of biological organisms and pathogens. Low relative humidities also tend to dry the mucous membranes and the skin which can lead to chapping and irritation. High relative humidities can cause a lack of evaporation from the skin when exposed to high temperatures. This lack of evaporation can lead to heat exhaustion and heat stroke. The relationship between health and relative humidity is illustrated in Fig. 1. Therefore, rather than to eliminate moisture in living environments, the prime motivation for the study of moisture diffusion in buildings is to better understand and model the phenomena to develop methods to control the moisture buildup in structural members and insulation and predict when the recommended relative humidity for health exceeds the humidity tolerance of the building structure

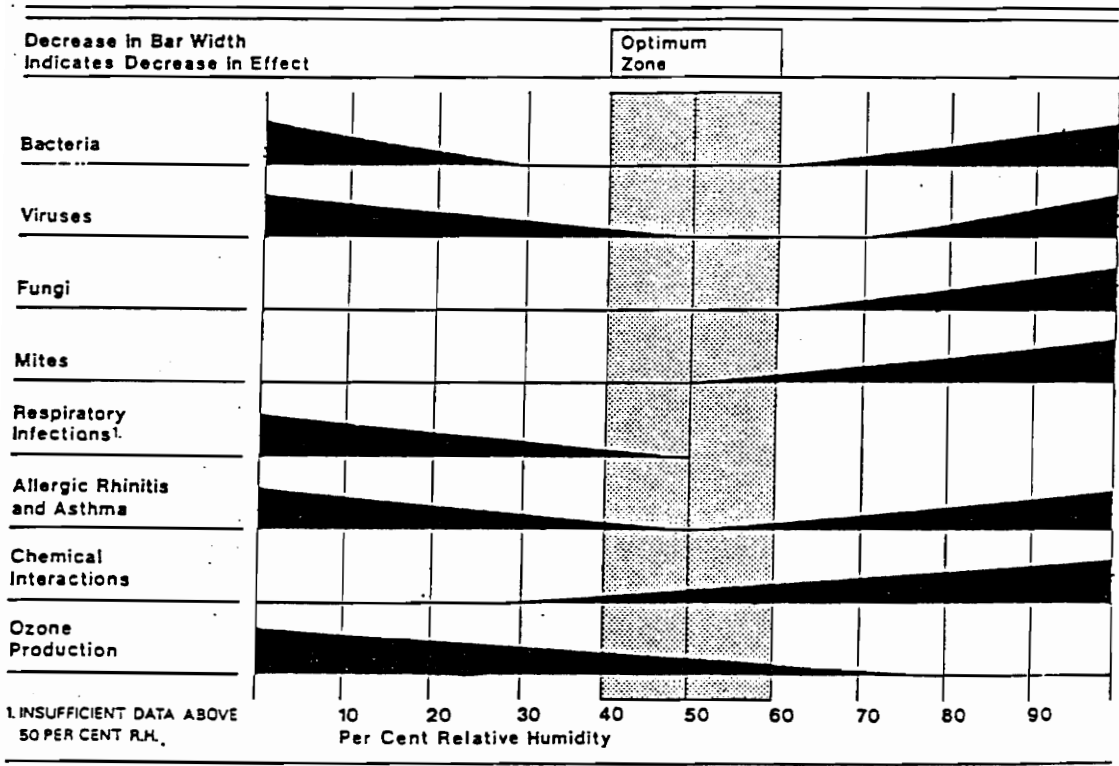


Fig. 1 Optimum relative humidity ranges for health (Sterling et al. 1985)

(Tenwolde, 1989). Better moisture control will thus help prevent mold formation and structural damage and help promote energy conservation.

There has been a good deal of study concerning mathematical modeling of mass diffusion. An underlying problem in developing an accurate model is the lack of abundant, credible data with which to test and refine models. The testing methods used for data collection generally consist of some method of maintaining a relative humidity difference across a specimen material under a certain temperature condition and measuring the moisture diffusion through the specimen. These tests normally are carried out under isothermal conditions (in which the temperature on each side of the specimen is the same) and the relative humidities are varied.

A considerable amount of data has been collected under isothermal conditions using the testing methods discussed in section 1.1.1. These data, however, have been called into question.

There is a significant lack of data in which the temperature on each side of the specimen is different.

1.2 Test Methods

A standard test for measuring moisture transfer in porous materials is prescribed by the American Society of Testing and Materials (ASTM, 1988). Other test methods have been developed by individuals. Several of these testing methods will be discussed.

1.2.1 ASTM Standard Test

The standard test method for testing moisture transfer properties of materials is ASTM 96-80. Two basic methods make up the standard: the Desiccant Method and the Water Method, also known as the dry cup and the wet cup methods, respectively.

An example of such a test is represented in Fig. 2. In each test, there is a test chamber (1) into which a test dish (2) is placed. A specimen material (3) is sealed into the mouth of the test dish with wax. Inside the test dish is placed a desiccant or saturated salt solution (4) depending on the desired test conditions. Inside the test chamber, surrounding the test dish can be placed another saturated salt solution (5). The ASTM standard only mentions using distilled water and desiccant, however, saturated salt-in-water solutions are normally used to give a certain relative humidity in the test atmosphere.

Saturated salt solutions yield a certain relative humidity by affecting the water vapor pressure over the solution. If a certain salt is maintained in solution such that a portion is in the solid state, then the solution is saturated and a constant vapor pressure, characteristic of the particular salt being used, will be maintained. As moisture diffuses into the test environment containing the saturated salt solution, the solid salt will dissolve proportionally to maintain the proper moisture content of the air. If moisture is lost from the testing environment in the vapor phase, then evaporation from the liquid takes place and a proportional amount of salt will

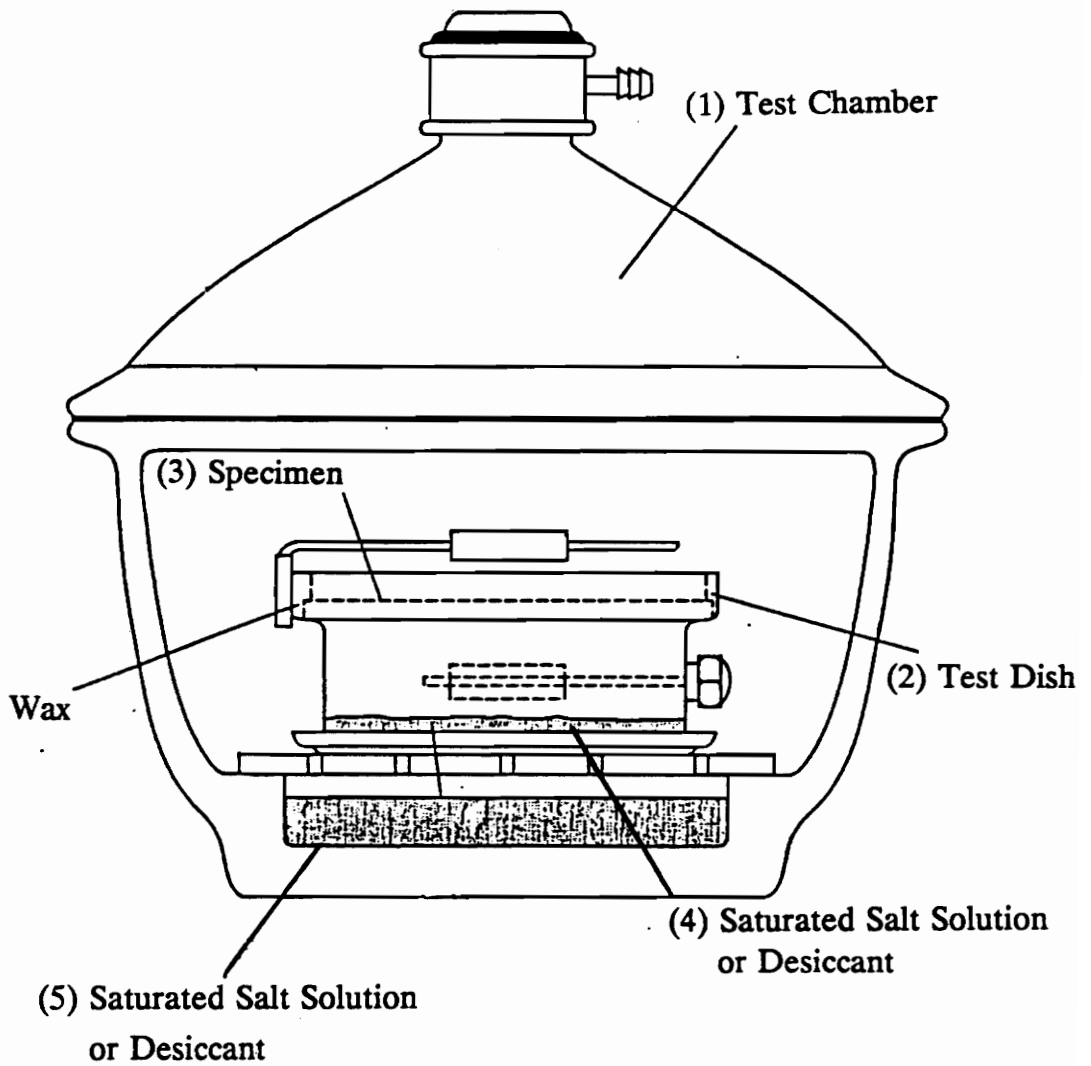


Fig. 2 Typical ASTM 96-80 testing apparatus

precipitate out of solution. Depending on the salt that is used, many different relative humidities can be obtained (Fanney et al., 1991).

To measure the moisture diffusion rate, the specimen dish is removed periodically and weighed. When the weight change of the dish and specimen remains constant in successive measurements, then steady state conditions have been reached and the steady state diffusion rate can be determined.

The advantage of the cup method is its simplicity. The test can be carried out with a minimum of equipment and with little effort after the test is running.

The disadvantages are the salt solutions used for humidity control, the necessity of removing the specimens for weight measurements, and the temperature effects of the evaporation and condensation of the water in the test chambers. These disadvantages are explained in the following paragraphs.

When saturated salt solutions are used for humidity control, the salt in the vapor phase tends to migrate to the surface of the specimen. The salt is suspected to effect the diffusion characteristics of the specimen material and thus cause errors in the data acquired.

When the specimen dish and specimen are removed from the controlled test environment for weight measurements, they will be exposed to a different set of environmental conditions which will affect the moisture content of the specimen and the test dish. Depending on the material being tested and the length of time of exposure, this exposure to the ambient could cause enough moisture gain or loss to

result in significant error in the data.

Finally, in the cup method, it is assumed, because the chamber and the specimen cup are together in the same temperature environment, that the test is carried out under isothermal conditions. There is, however, doubt concerning the validity of this assumption. As the water vapor is absorbed into the specimen, there is heat of sorption released at the surface of the specimen which tends to elevate the temperature at the interface. On the other side of the specimen, the energy to evaporate the moisture diffusing through the specimen tends to depress the temperature at this surface. This phenomenon has the potential to void the isothermal assumption for the test.

1.2.2 Other Methods

Tveit (1966) outlined a method used for testing the moisture permeability of porous materials that in many ways resembled the ASTM standard test, but it had some notable differences. The testing apparatus, as shown in Fig. 3, consisted of an environmental chamber (1) in which air circulated over a heat exchanger (2) for temperature control and through a salt solution (3) for humidity control. The trays in which the specimens were sealed (4) were placed on an elevator (5) from which they could be removed periodically and weighed on a scale. The scale (6) was placed on top of the apparatus and had a hook which extended into the chamber through a hole. In this manner it was not necessary to remove the specimen cups from the controlled environment.

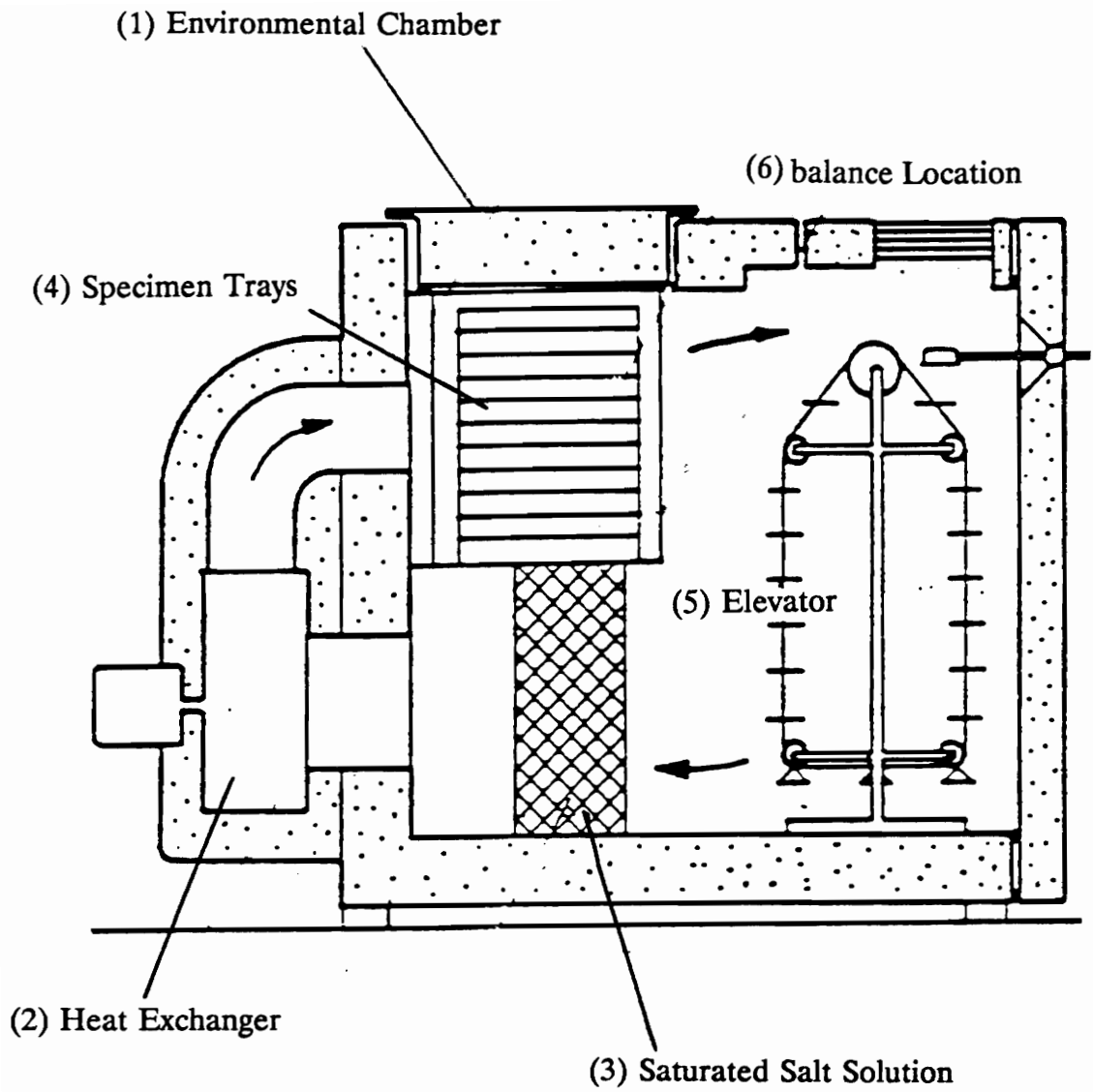


Fig. 3 Tveits (1966) moisture diffusion testing apparatus

The advantage of this method over the ASTM standard test was the ease of performing tests at different temperatures. It was also advantageous to be able to weigh the specimens without having to remove them from the chamber.

The disadvantage was the use of salt solutions to maintain relative humidity. This usage brings up the same concerns as are discussed with the ASTM test. This test method is also restricted to isothermal tests.

Another method of moisture diffusion measurement was developed by Douglas (1991) for nonisothermal as well as isothermal conditions. His apparatus, shown in Fig. 4, consisted mainly of two large pots (1) wrapped individually with copper cooling coils (2). Between the pots, a specimen (3) was sealed. Inside each pot (not shown) were a saturated salt solution on an electronic balance, a relative humidity sensor, and a fan. The relative humidity was maintained by the saturated salt solution on the balance. The relative humidity sensor was used to monitor the relative humidity within the chamber. The fan was used to create forced convection to facilitate mixing of the air and moisture in the chambers. Temperature was controlled by circulating cooling or heating solution through the copper coils which were wrapped around the chambers. The moisture diffusion measurement method was to measure the weight gain of the solution on the electronic balance over a period of time.

The disadvantages of Douglas' approach are the use of salt solutions for humidity control and locating the electronic balance within the test chamber.

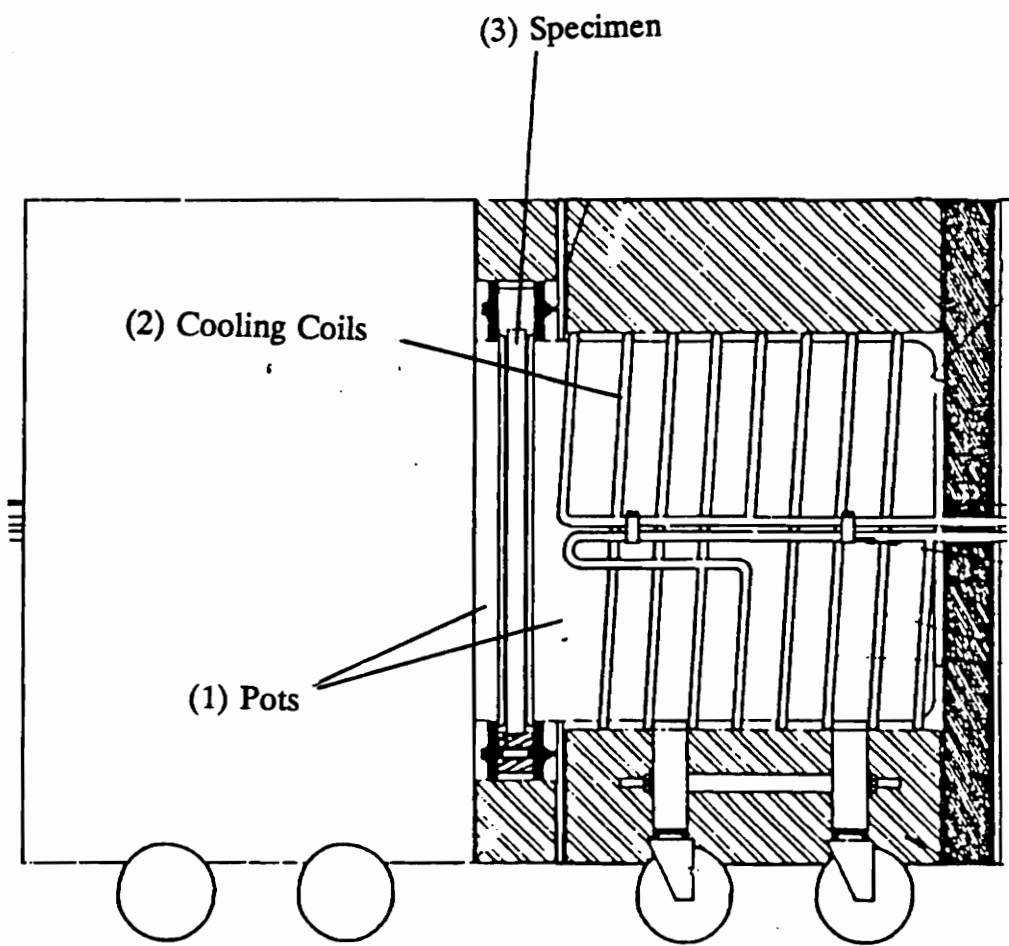


Fig. 4 Douglas's (1991) moisture diffusion testing apparatus

Instrument drift over time could cause error in the data.

1.2.3 Shortcomings of the Test Methods

The problem with all the methods, except the one by Douglas, is the inability to perform nonisothermal tests.

A weakness that all the previous test methods have, is the usage of salt solutions for relative humidity control. There is a possibility that salt solutions pose no problem, but until sufficient tests have been done which do not use this saturated salt-in-water solutions to compare results, it remains suspect.

1.3 Objectives of the Research

The main objective of the present research was to develop a detailed design of an improved device to measure moisture diffusion in various building materials under nonisothermal and isothermal conditions. The general criteria of this apparatus were independently variable relative humidity and temperature differences on each side of a specimen material without the use of salt solutions.

1.4 Target Operating Limits

The target ranges of operation were chamber temperatures from 5°C to 60°C, controlled to within $\pm 1^\circ\text{C}$, with the capability of having a temperature difference across the specimen of 20°C over the temperature range. The relative humidity target limits were 10 to 90 percent, controlled to within ± 2 percent relative humidity.

II. Apparatus

The present objective was to design the apparatus. In order to verify the design, the temperature and relative humidity control systems, and the diffusion rate test system were built and tested. The air circulation system was also tested and recommendations are made concerning this part of the system.

This section gives an overview of the entire system and its operation. Detailed descriptions of individual components of the system are presented later.

2.1 Overview

The experimental apparatus, illustrated in Fig. 5, consists of dual environmental chambers. The test specimen is sealed in a specimen holder which fits between the open ends of the chambers. Air is conditioned external to the chambers for temperature and moisture control. The air is circulated through the chambers with an external pumping system.

The moisture content of the environment is controlled by using desiccant and water-filled columns. The desiccant column consists of a tube filled with a drying agent through which air is passed to remove moisture. The water-filled column, referred to as a bubble column, is a cylinder, partially filled with water, through which the air is bubbled for humidification. The moisture which transfers through the specimen from one chamber to the other is absorbed in a desiccant column to maintain the desired relative humidity in the test environment. The bubble column is used to replace the moisture to the test chamber which loses moisture during

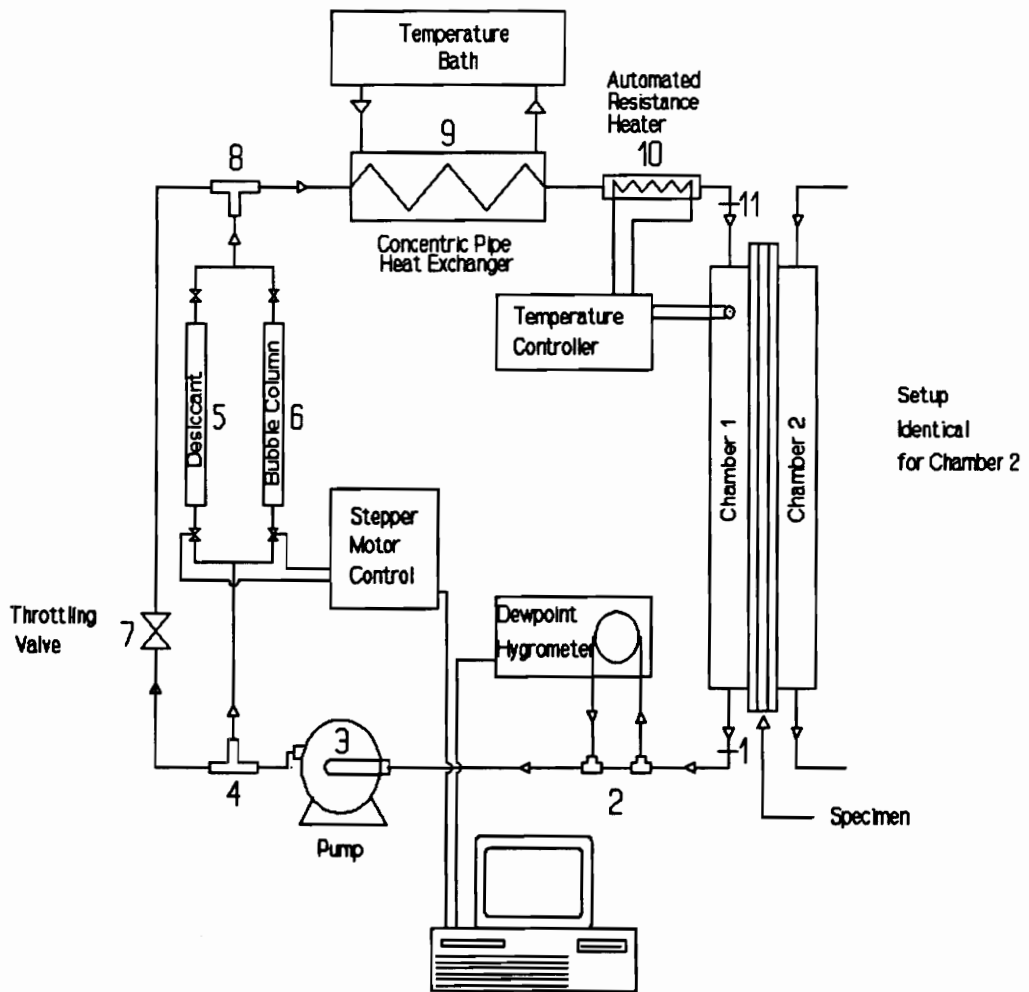


Fig. 5 Overview of the apparatus

moisture transfer through the specimen. The desiccant and bubble columns are also the mechanisms by which the moisture transfer rate is determined. Moisture transfer rates are determined by measuring the weight change of the columns over time.

The chamber air temperature is controlled with heat exchangers and automatically controlled electrical resistance heaters.

2.2 Operation

Referring to Fig. 5, the system operation is described starting at the exit point of the chamber. Air leaving the chamber (1) is immediately sampled to determine its moisture content (2). The sample lines are two small tubes, one leading to a dewpoint hygrometer and one leading back to the main flow. The dewpoint temperature is monitored to determine if any adjustments should be made to the moisture content of the air entering the chamber. Air flows through the pump (3) to the bypass fitting (4). At this point, a small amount the air is routed through the desiccant (5), or the bubble column (6), depending on whether moisture needs to be added or removed. The main flow is bypassed through (7) to (8). The air streams are mixed at (8). A throttling valve at (7) insures that there will be enough pressure to force the air through the desiccant and bubble columns.

The air is next cooled or heated by passing through the water-to-air heat exchanger (9) and electrical resistance heater (10). The heat exchanger heats or cools the air to a few degrees below the desired temperature. The resistance heater, placed between the heat exchanger exit and the chamber entrance, automatically

controls the temperature to the desired temperature value of the chamber (11).

The method for determining the moisture diffusion rate is by measuring the weight change of the desiccant on the moisture gain side over a given time interval. The water weight loss in the bubble column on the moisture loss side can also be measured as a check. The desiccant and bubble columns are fitted with quick-disconnect fittings to rapidly remove and install the columns in line. Self-sealing fittings prevent leaking when the tube is removed.

2.3 Design

2.3.1 Modelling the Apparatus

After design conception, computer models were developed to help determine design parameters. The parameters were size of the chamber, size of heat exchanger, recirculating air flow rate, thickness of insulation, and amount of flow through the desiccant and bubble columns. In order for these parameters to be determined, it was necessary to estimate the heat transfer load on the chamber and the diffusion rate through the specimen materials.

One of the models was an isothermal moisture diffusion model for porous materials. This model provided the ability to estimate the total moisture diffusion through a specimen. The two materials chosen for comparison were gypsum and white pine. The materials were chosen because they represent reasonable limits of moisture transfer rates and the diffusion coefficients are readily available. Gypsum is a highly porous material while white pine represents a less porous material. High

total moisture transfer, and thus a large specimen size, is desirable because higher weight gain or loss in the columns for a given time period results in less error in the measurements. Also, with higher total moisture transfer, more data points can be collected during a specific time period which statistically increases the accuracy of the measured diffusion rate. The moisture diffusion rate was calculated from the mathematical model developed by Thomas et al. (1990)

$$\dot{m}'' = \frac{\gamma_{s1} - \gamma_{s2}}{\frac{L}{\rho_d \bar{D}}} \quad (1)$$

where \bar{D} is a mean value. If the diffusion coefficient, D , is as chosen in the form

$$D = D_0 e^{a\gamma} \quad (2)$$

and the convective mass resistance on each side of the specimen is included, then the mass flux is

$$\dot{m}'' = \frac{D_v(\gamma_1) - D_v(\gamma_4)}{\frac{RT}{P_g h_m} \frac{D_v(\gamma_1) - D_v(\gamma_2)}{\phi_1 - \phi_2} + \frac{aL}{\rho_d} \frac{\gamma_2 - \gamma_3}{D_v(\gamma_2) - D_v(\gamma_3)} + \frac{RT}{P_g h_m} \frac{D_v(\gamma_3) - D_v(\gamma_4)}{\phi_3 - \phi_4}} \quad (3)$$

The convective mass transfer coefficient, h_m , was determined by (Incropera et al., 1985)

$$h_m = h \left(\frac{D_{AB} L e^{\frac{2}{3}}}{k} \right) \quad (4)$$

The vapor mass diffusion coefficient, D_{AB} , was obtained from Thomas et al. (1990).

The Lewis number is calculated from

$$Le = \frac{k}{\rho C_p D_{AB}}$$

The complete moisture diffusion model is listed in Appendix 1. The diffusion coefficients for gypsum and white pine were obtained from a paper by Fanney et al. (1991). Values of the diffusion coefficients at temperatures of 24.4°C (76°F) and 6.67°C (44°F) were used.

The range of air flow rates and cooling or heating loads needed to maintain the desired chamber temperature were found from the heat transfer simulation. The model was developed from energy balances on the apparatus.

An important concern addressed with the heat transfer model was the trade off between having the specimen large, in order to have maximum total moisture transfer for measurement purposes, and higher heat transfer loads resulting from the large size. Moisture diffusion is a relatively slow process except for the most porous materials. It can take months to obtain steady state data with some materials using the ASTM testing procedure (Thomas et al., 1990). It was therefore desirable to make the specimen have as large a surface area as possible to increase the total moisture transfer so measurements could be taken within a reasonable period of time, e.g., preferably two or three measurements a week. The problem with making the specimen surface area larger was that the chamber had to be bigger which resulted in more area for heat transfer, thus increasing the overall load. Heat

transfer loads impose limits on the temperature and relative humidity operating ranges that are challenging to overcome as will be shown in chapters III and IV.

A concentric tube heat exchanger design program was also written to determine the necessary heat exchanger tube lengths considering the loads indicated from the system design simulation.

2.4.2 Choice of Materials

Low moisture absorptance and low thermal conductivity are criteria in choosing materials for building the apparatus. Low thermal conductivity is desirable for lower heat losses or gains. Low moisture absorptance is essential for minimum measurement error. All moisture transferred through the specimen should be absorbed in the desiccant. Moisture absorbed in any other part of the system results in error in determining the mass transfer rate.

Rigid acrylic tube and sheet are the materials chosen for the chambers. It is chosen for its low thermal conductivity, transparency, and low moisture absorption. The ability to see the specimen through the chamber is advantageous in case of unexpected condensation which would lead to error in the weight measurements, and for visual inspection of the specimen itself.

ImpoleneTM tubing is used for the piping system. Impolene is a thermoplastic which consists of a mixture of polypropylene and polyethylene. This tubing is recommended by the dewpoint hygrometer manufacturer for the sampling system so it was used for the entire piping system. The advantages of Impolene are its

relatively low thermal conductivity, low moisture absorption, and ease of use.

Acrylic tubing is used for the bubble columns. The desiccant columns are constructed from thin-walled brass tubing.

A rubber foam type insulation was used to insulate the chambers and portions of the piping. This material is used because it insulates well and is easy to apply. It has a nominal thermal conductivity of approximately $0.0344 \text{ W/m}^{\circ}\text{C}$.

2.4.3 The Chambers

After choosing acrylic tube as the chamber material, it was necessary to determine the sizes needed for maximum moisture diffusion without excessive load. The dimensions chosen for the environmental chambers are shown in Fig. 6. These dimensions were chosen with the moisture transfer given the most consideration. It was accepted that heat loads on the chamber could be resolved easier than problems with low moisture transfer of specimen materials. Flanges are cut such that they press fit onto the outside of the chamber tube section and are sealed to the chamber wall using a solvent cement. The endplates are sized such that they press into the chamber tube section and are sealed into place. The construction of the flanges and endplates is also shown in Fig. 6. Insulation is placed around each chamber, 0.0508 m (2 in.) thick, up to the flange. The entire chamber setup is covered with 0.0254 m -thick (1 in.) of insulation.

The gasket material chosen to seal the specimen holder between the chamber

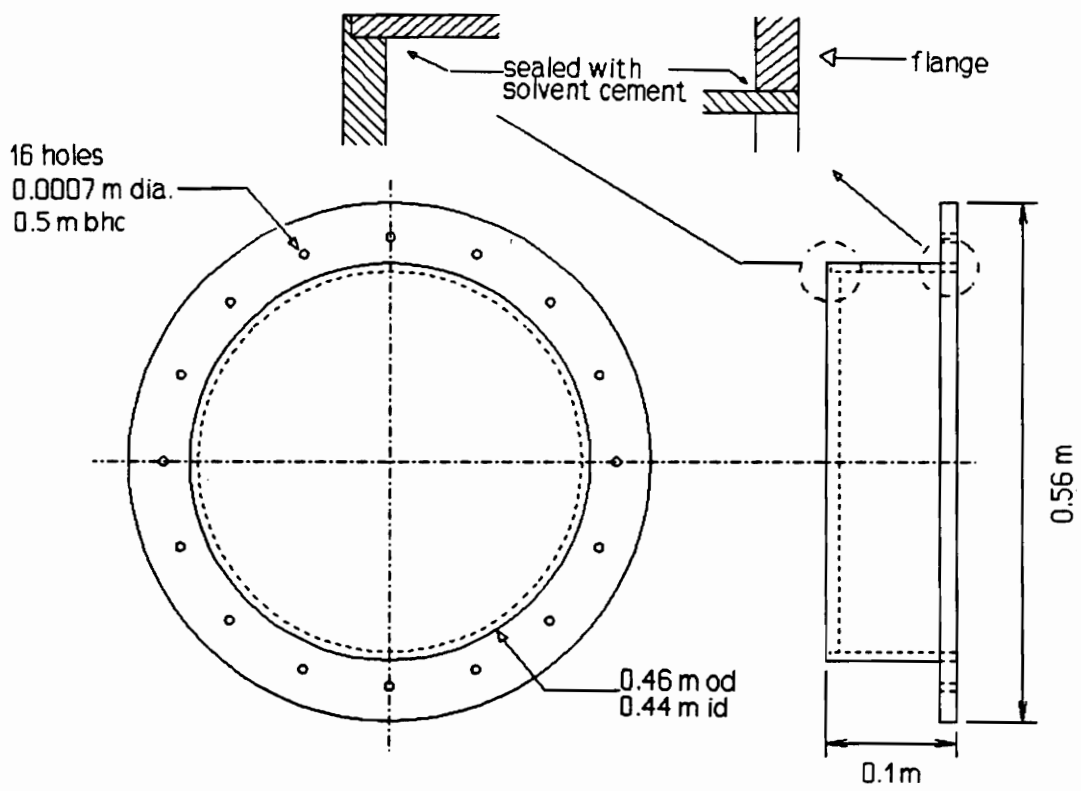


Fig. 6 Dimensions and construction details of the environmental apparatus

is nitrile rubber with an A40 hardness. This rubber has low vapor diffusivity, excellent resistance to moisture sorption and swelling, good pliability, and reasonable cost. It is chosen with a thickness of 3.175 mm (1/8 in.). The thickness coupled with the softness gives a good seal that compensates for small irregularities in the flanges and chamber edge.

The two inlets to the chamber are placed opposite each other in the tube wall as shown in Fig. 7. The outlet is placed in the center of the endplate. To improve mixing in the chamber, the pipe thread end of each inlet fitting is drilled out and an injector is press-fitted into it such that it protrudes into the chamber. The injectors are illustrated in Fig. 7. The outlet is illustrated in Fig. 8.

The specimen holders are cut from acrylic sheet of various thicknesses, as shown in Fig. 9. The specimen is cut to size and sealed in the holder with a 60/40 mixture of microcrystalline and paraffin wax. This wax is recommended in ASTM E96-80 for the following reasons:

1. Impermeable to water in either vapor or liquid form.
2. Experiences no gain or loss of weight from or to the test chamber (evaporation, oxidation, hygroscopicity, and water solubility being undesirable).
3. Good adhesion to any specimen and to the specimen holder even when wet.
4. Complete conformability to a rough surface.
5. Compatible with the specimen and has no excessive penetration into it.
6. Strength or pliability (or both)
7. Easy handleability (including desirable viscosity and thermal of molten sealant)."

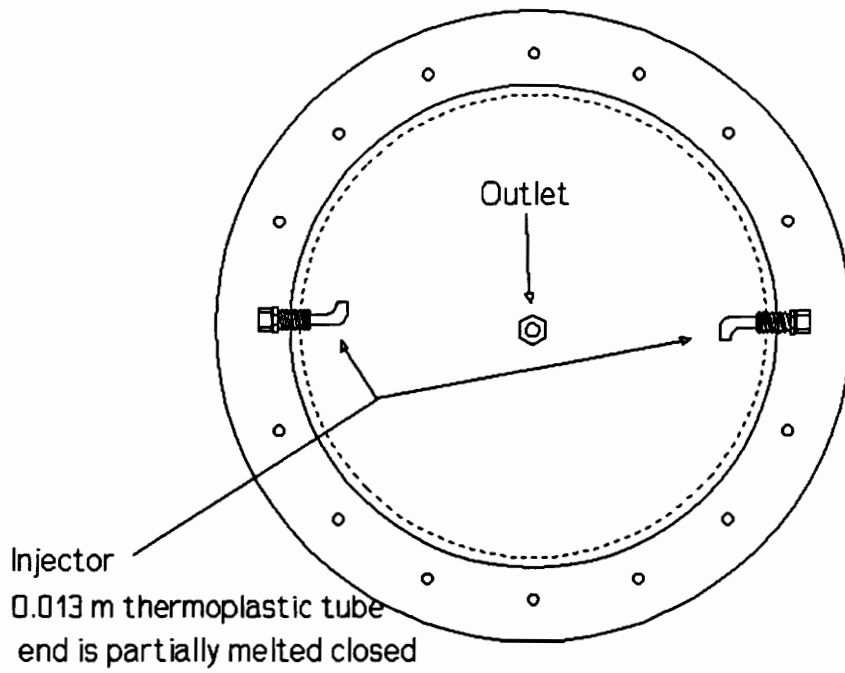


Fig. 7 Injector inlets

Side View of Chamber

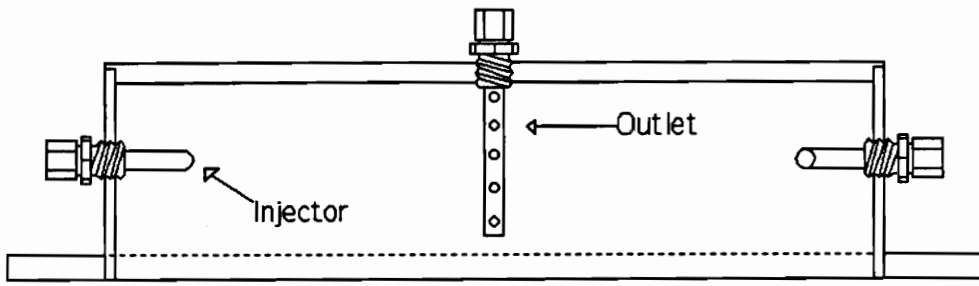


Fig. 8 Chamber Outlet

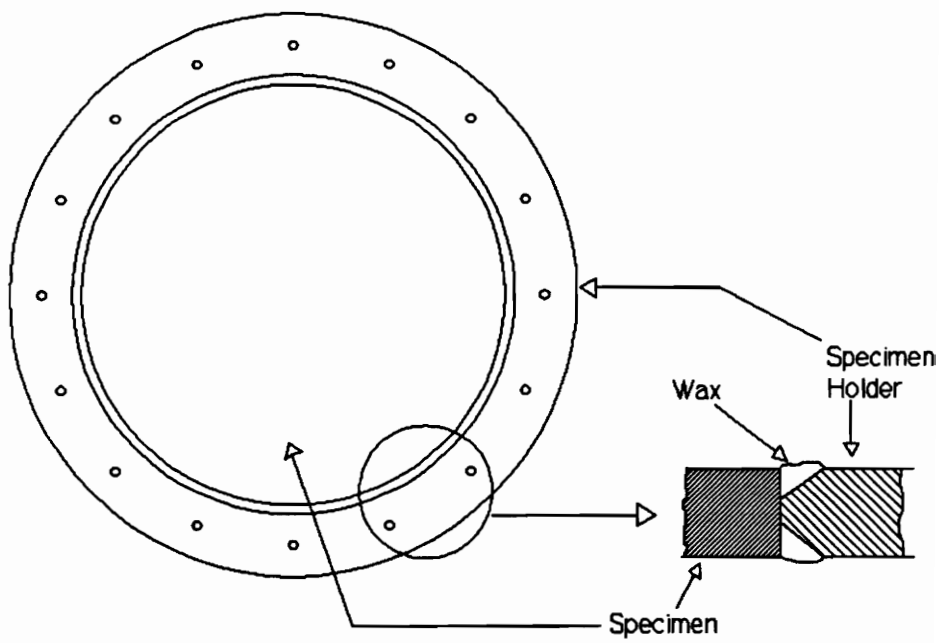


Fig. 9 Specimen holder

The wax must completely cover the outer edge of the specimen without spilling over on the face of the specimen which would cause uncertainty in the effective specimen area.

The present chamber allows for specimens of various diameters up to 0.43 m (17 in.). In order to use smaller specimens it would be necessary to use a specimen holder with a different size mounting hole. The reasons for using a smaller specimen would be specimen size availability or when using a material of high moisture diffusivity where the desiccant could saturate too quickly. It is also possible that noncircular specimens could be used by constructing a specimen holder with a hole corresponding to the specimen shape.

The chamber temperature measurement system consists of thermocouples placed at the entrance, exit, and interior of the chamber. The thermocouple fittings are shown in Fig. 10. The thermocouple readings are taken by a Hewlett-Packard (HP) model 3497A Data Acquisition system which is controlled by an IBM-Compatible PC equipped with an HP-IB card.

2.4.4 The Desiccant and Bubble Columns

The recirculating air, as it is pumped from the chamber, has an excess or a shortage of moisture relative to the desired test conditions because of the moisture gain or loss from diffusion. Therefore, in order to restore the desired moisture content to the air, a method of moisture control is necessary.

The method of moisture control employed is to continuously remove a fraction

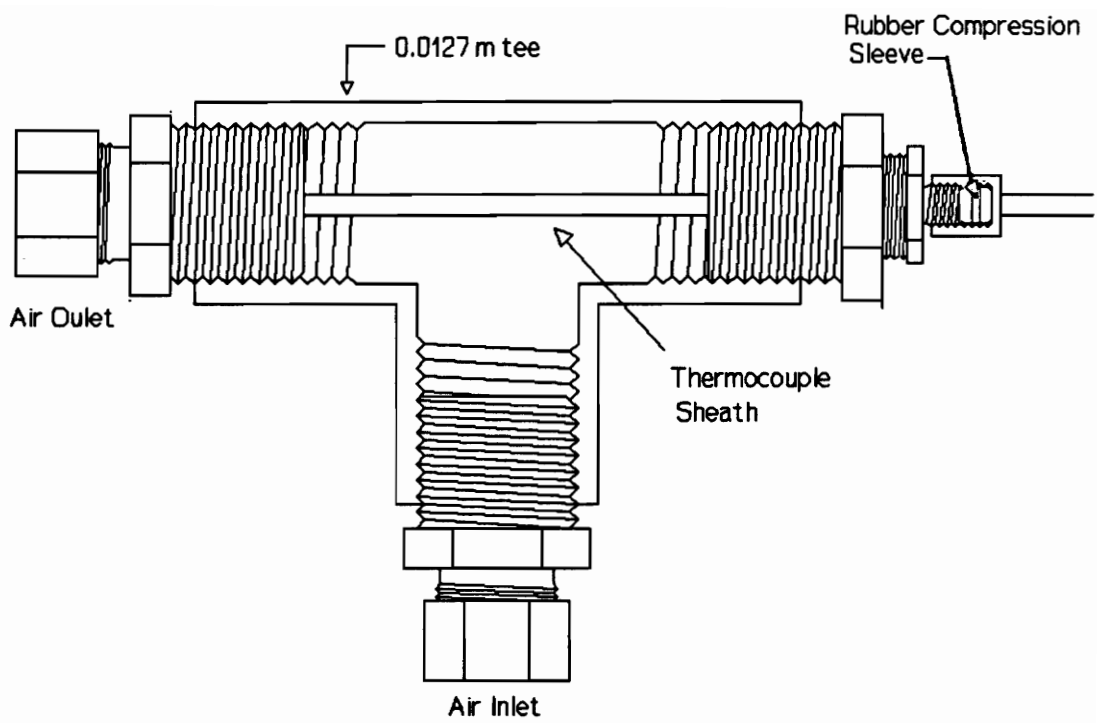


Fig. 10 Thermocouple fittings

of the flow and either dry it, or humidify it, and then return it to the main flow. The flow rate through the desiccant or bubble column should be sufficient to return the main air flow to the proper moisture content after mixing.

In addition to moisture control, the bubble and desiccant columns are also used for moisture diffusion rate measurements by weighing the weight change of the column over a chosen time interval. The electronic balance used has a resolution of 0.001 g and a maximum load limit of 410 g. The bubble and desiccant columns are designed to be light enough to be weighed with the available balance and large enough to operate a sufficiently long time before needing to be recharged.

The bubble column, illustrated and dimensioned in Fig. 11, consists of an acrylic cylinder with one brass quick-disconnect fitting in the top and one on the side. The air enters through the fitting on the top and flows to the bottom of the bubble column through a brass tube connected to the bottom of the fitting. The air bubbles through the water and is humidified. Preliminary tests showed that even for water columns as short as 50 mm the dewpoint of the air came to within 1°C of the water temperature which is approximately equal to the ambient temperature. The air then leaves through the fitting in the side of the column which is positioned near the top to help prevent liquid from splashing into the piping system. The approximate weight of the empty bubble column is 160 g and when half-filled with water weighs approximately 240 g.

The desiccant column, as shown in Fig. 12, consists of a vertical thin-walled

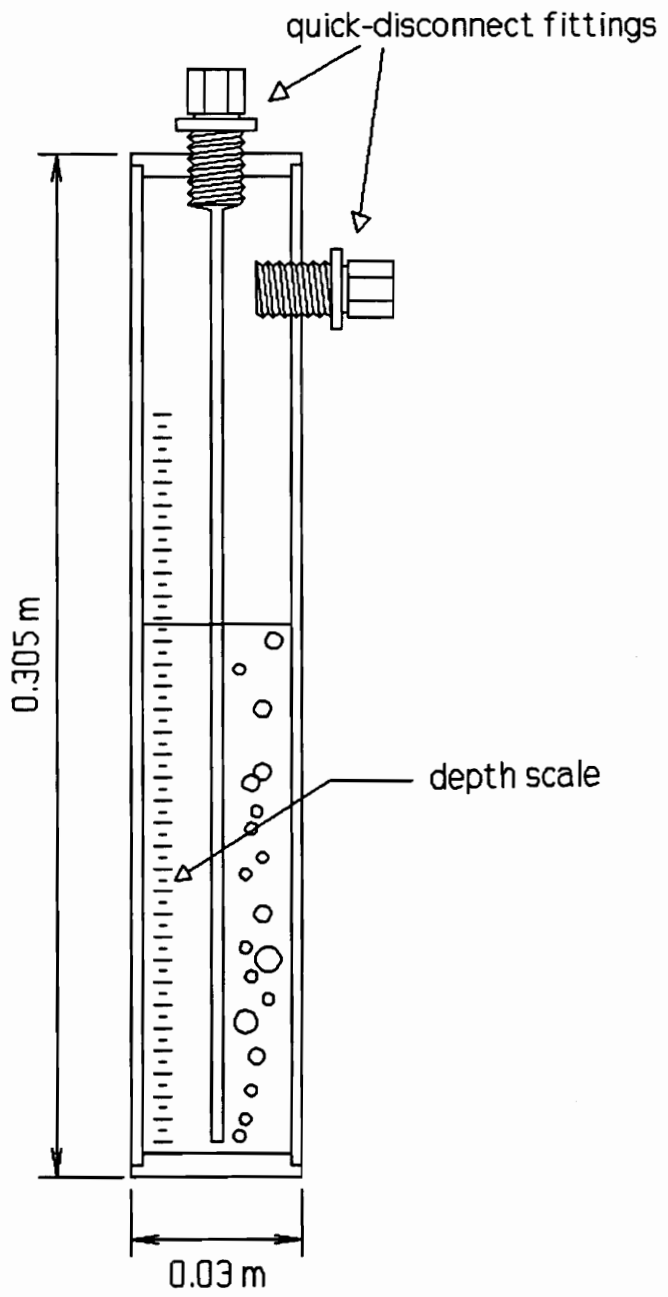


Fig. 11 Bubble column

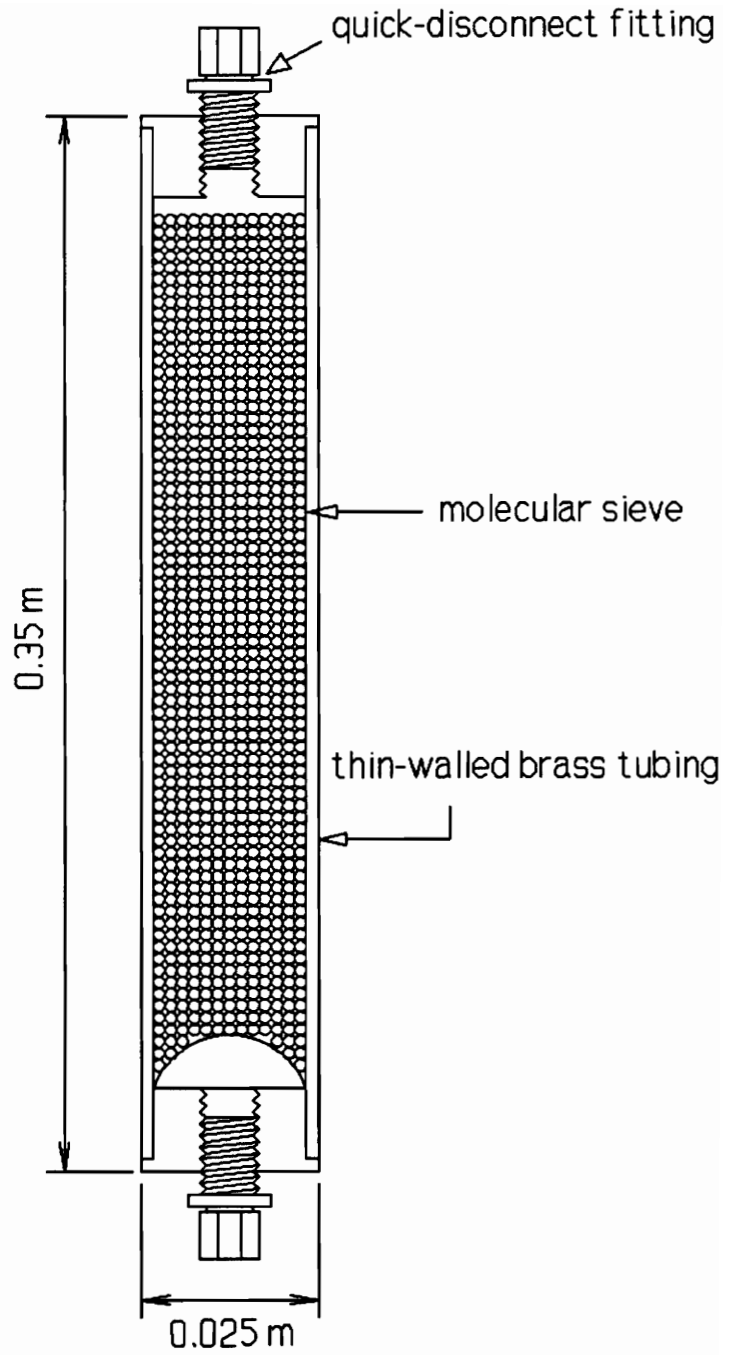


Fig. 12 Desiccant column

brass cylinder containing a molecular sieve with a 4 Å pore size as the drying agent. This particular molecular sieve is dry, light, chemically inert, and selectively absorbs water molecules. A quick-disconnect fitting is placed into each end of the desiccant column. It is important that the column stand vertically to prevent the drying agent from settling to one side, thus allowing the air to flow around, instead of through, the drying agent.

A series of tests were conducted to assist in determining the proper heights and weights of the desiccant column. As mentioned previously, the desiccant column is designed to be light enough to stay within the weight limits of the available balance yet have enough drying agent to operate a reasonable length of time before saturation. The height is also sufficient to properly dry the air. The tests involved pumping atmospheric air through various desiccant column heights and at various flow rates. The flow rates for the tests were equivalent to the estimated flow rates through the desiccant determined from a combination of the heat transfer model and the moisture diffusion model. Using these models it was possible to estimate the flow through the desiccant or bubble column from the amount of moisture diffusing through the specimen. The flow rates were divided by the cross-sectional area of the tube and the results are presented as a function of flow per unit area. The results of the tests are included in Appendix 2.

Using the data collected, it was possible to estimate the size of the desiccant column required for most test materials and conditions. The size chosen for the

desiccant columns is shown in Fig 12. The dry weight is approximately 360 g. The operating time to saturation of the desiccant column will depend on the moisture diffusion through the specimen. The desiccant can be recharged more often when testing materials of high diffusivity, or in the case of very high diffusion rates, a smaller specimen could be used.

Both chambers are equipped with bubble and desiccant columns to speed up the process of coming to the target test conditions. Start up will often begin at ambient relative humidity, and the target moisture content of either chamber may be at, above, or below ambient moisture content.

The control of relative humidity using the desiccant and bubble columns is automated with a pair of metering valves driven with stepper motors that have a resolution of 200 turns per revolution. The code which drives the motors is a proportional-integral (PI) control algorithm. Readings from the dewpoint hygrometer are imported through the HP 3497A controller, and adjustments are made to the metering valves as needed to maintain a desired dewpoint temperature.

2.4.5 The Heat Exchangers and Resistance Heaters

The purpose of the concentric tube heat exchanger is to cool or heat the fluid to approximately 1°C to 4°C below the desired inlet temperature of the chambers. The temperature is then precisely controlled using an automated electrical resistance heater.

The concentric tube heat exchanger is constructed using copper tube, and

brass pipe fittings as shown in Fig. 13. The cooling fluid passes through the outer tube, and the chamber air passes through the inner tube. The advantage of making the heat exchangers in this manner is that it can be done quickly and modifications are relatively easy. If longer tube sections are desired it is only necessary to remove the old sections and install the new ones. The inlets and outlets of the heat exchanger for both the cooling fluid and the air are fitted with thermocouple fittings to facilitate temperature measurement when desired.

Analysis determined that for a load of approximately 30 W (estimated from the heat transfer model) and a flow rate of $0.05 \text{ m}^3/\text{min}$, a 0.76 m to 0.914 m heat exchanger length would be sufficient for the tube sizes shown in Fig. 13.

The automated resistance heaters are constructed from copper tube and 50 W heating elements as shown in Fig. 14 and are placed in line between the heat exchanger and chamber. The heating elements are supplied a voltage from a Eurotherm™ PID temperature controller which continuously monitors the temperature at a control point and adjusts the voltage as necessary to maintain a constant temperature. The controller is capable of maintaining temperatures to within 0.1°C of the setpoint.

The cooling fluid for the heat exchanger is provided by a Forma Scientific model 2425 constant temperature bath. This bath allows a cooling and heating range from -34°C to $+76^\circ\text{C}$.

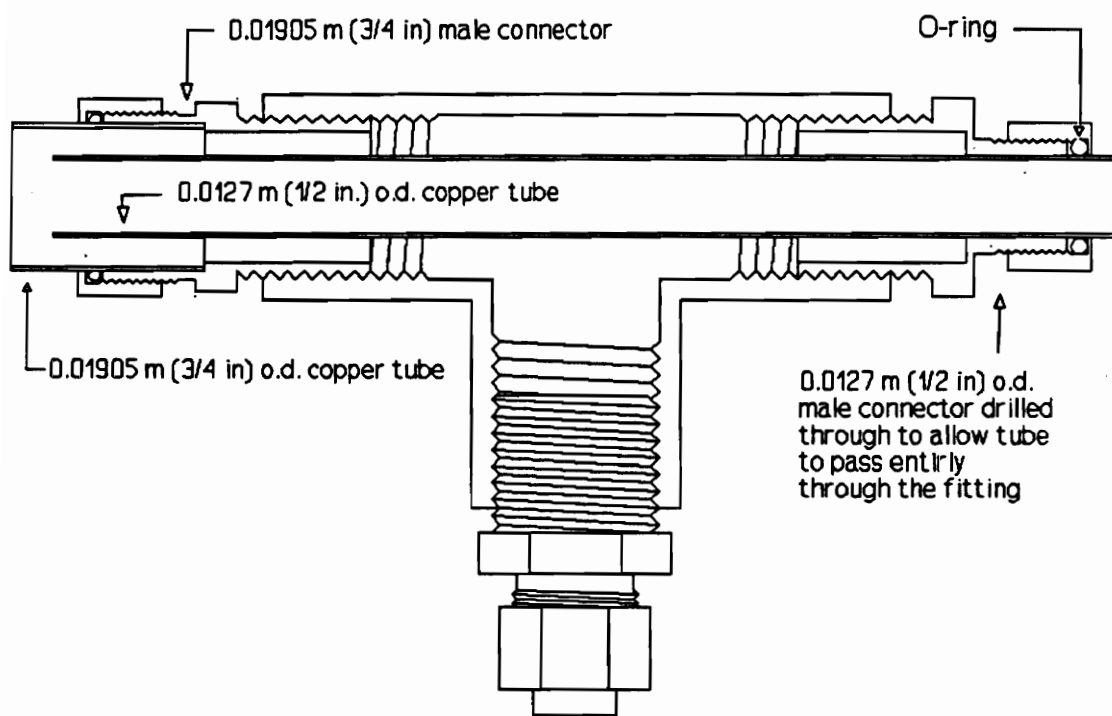


Fig. 13 Concentric tube heat exchanger connections

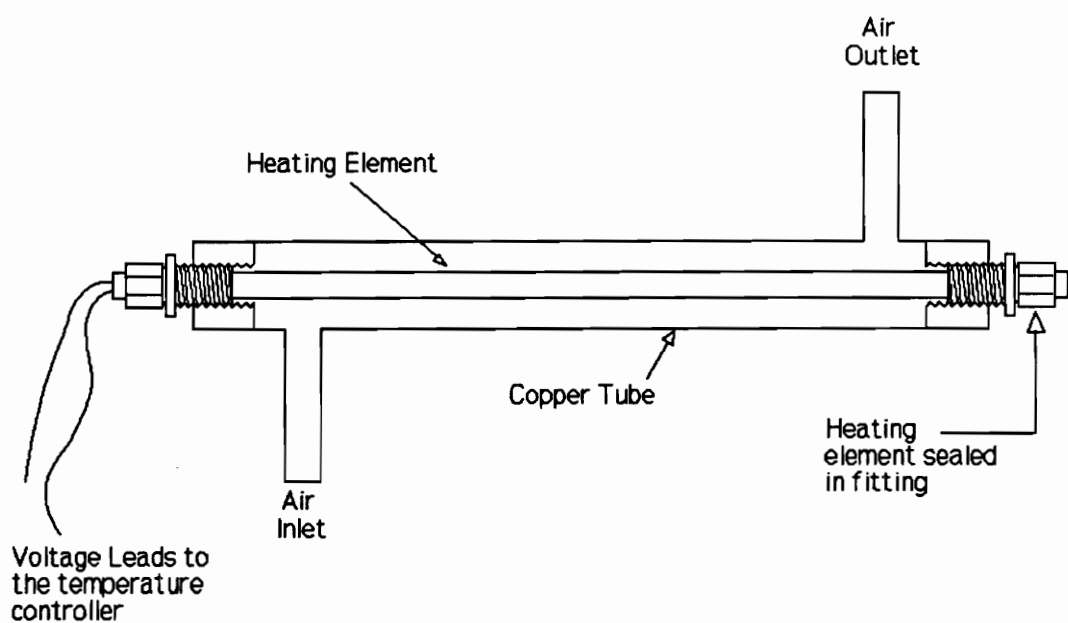


Fig. 14 Automated resistance heaters

2.4.6 The Sampling System

The sampling system consists of a bleed-off section immediately after the exit of the chamber as shown in Fig. 5. This section consists of two small tubes which lead to and from the main air line. The sample air is considered representative of the chamber air because the moisture content of the air in the chamber is assumed uniform from mixing. The sample of air is taken and routed through a General Eastern series 1311 sensor of a General Eastern 1200 APS Dewpoint Hygrometer. This system can continuously monitor air dewpoints as low as -65°C .

2.4.7 Pump system

The pump system consists of several diaphragm pumps connected in parallel. These pumps were chosen because they were believed to be leak resistant. Diaphragm pumps also tend to heat the air less than other types of pumps, thus reducing the required size of the heat exchangers. However, because of leak problems, which will be discussed later, these pumps were used to verify the operation of other parts of the system, such as the temperature control and the relative humidity control, but are not part of the final apparatus. Experience with these pumps also assisted in determining a satisfactory circulation system which will also be discussed.

III. Results

Throughout the presentation of the results the primary test chamber will be referred to as chamber 1 and the opposite chamber as chamber 2.

3.1 Isothermal Diffusion Simulation

Three different relative humidity operating conditions were used to calculate the moisture transfer across white pine and gypsum specimen of 0.43 m (17 in.) diameter and 0.013 m (0.5 in.). The differences ranged from 30 to 70 percent with average values of 30 to 45 percent. The results are shown in Table 1. The moisture diffusion rate for white pine is a factor of ten less than the gypsum for the highest rate of diffusion for white pine and the lowest rate for gypsum. As stated previously, the electronic balance has a resolution of 0.001 g. Therefore, at least 0.02 g of moisture has to be absorbed by the desiccant column or lost by the bubble column for a maximum uncertainty of 5 percent based on least-count. Figure 15 shows the times necessary to diffuse 0.02 g of moisture. These results are obtained from the worst case data from the diffusion simulation (Table 1). The white pine will diffuse 0.02 g of moisture in about 2.5 hours. These results show that the mass transfer rate measurement method, with the desiccant and bubble columns, is a feasible technical approach.

3.2 Thermal Characteristics of the Chambers

The heat transfer characteristics of the chambers were determined, by calculations and measurements, for isothermal and nonisothermal operating

Table 1: Results of the moisture diffusion simulation for white pine and gypsum.

Relative humidity Cham 1 Cham 2		White Pine		Gypsum	
		24.4°C g/day	6.67°C g/day	24.4°C g/day	6.67°C g/day
10%	50%	48.6	9.9	.48	.18
50%	80%	37.4	9.7	.94	.32
10%	80%	73.8	17.8	.7	.24

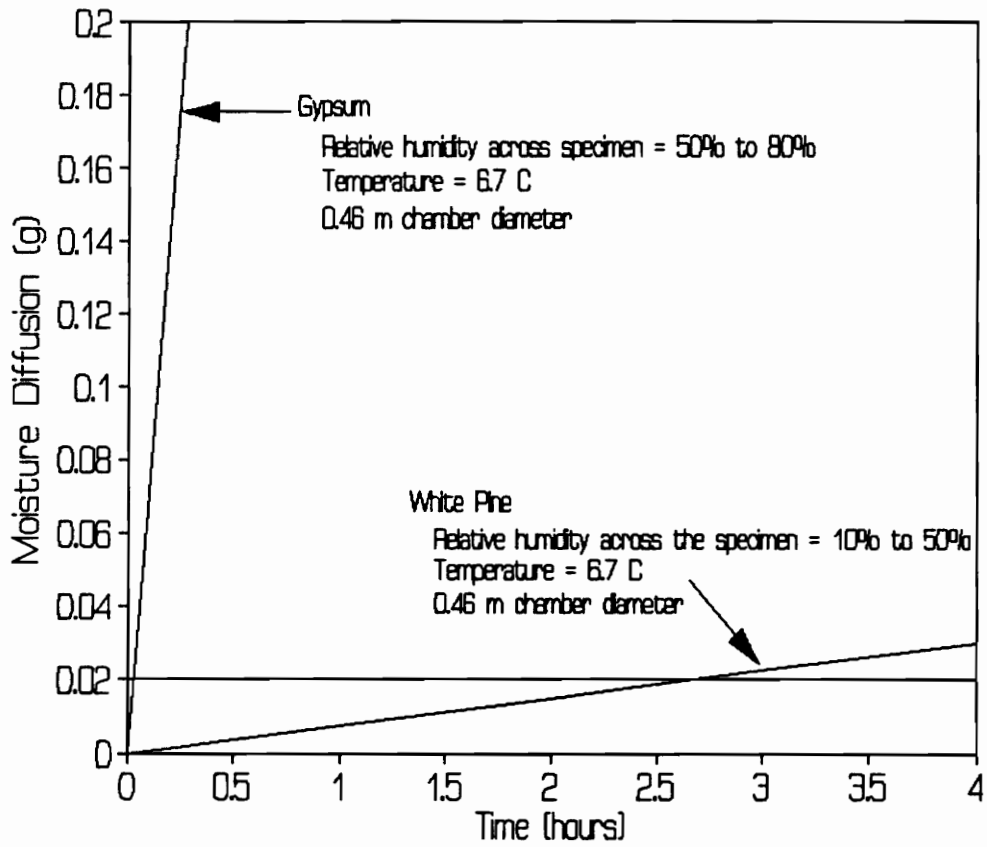


Fig. 15 Total moisture transfer vs time for a chamber with a diameter of 0.46 m.

conditions. The measured data are system specific. If any change is made to the insulation, flow rate, ambient temperature, or specimen material, the entire heat transfer rates will, of course, be changed. The equations used for the calculations predict performance accurately, and therefore, can be used to predict the performance of the chambers should an independent variable be changed.

The isothermal and nonisothermal heat transfer test results are presented in graphical form with the total heat transfer into (+) or out of (-) the chamber as the dependent variable. The heat transfer into or out of the chamber was determined from

$$q = \dot{m}C_p (T_o - T_i) \quad (6)$$

In the isothermal case, the heat transfer is plotted against the average chamber temperature. In the nonisothermal case the heat transfer is plotted against the temperature difference between the two chambers.

The heat transfer relation used was

$$q = UA (T_a - T_c) \quad (7)$$

The overall heat transfer coefficient, UA, was determined by treating the two sides and the circumference as parallel conductance paths. After determining UA, including the shape factor to account for two-dimensional effects at the corners, the resulting equation was

The experimental and calculated results for the isothermal case are compared in

$$q = .34 \frac{W}{^{\circ}C} \times (T_a - T_c) \quad (8)$$

Fig. 16. The average difference between the calculated and measured values of the heat transfer rate is 4.4 percent. The chambers were well insulated which results in the chamber inlet and outlet temperatures differing by only about 3 degrees for the chamber temperatures of 5°C and 42°C at an ambient of 24°C. At higher air flow rates, the temperature difference would be even less which would result in a more uniform chamber temperature.

The equation which describes the nonisothermal case began by taking the same heat transfer relation for a heat exchanger as used for the isothermal test, Eq. 6, and separately adding the heat transfer across the specimen. The result is

$$q = UA_{c1} (T_a - T_{c1}) + UA_{spec} (T_{c2} - T_{c1}) \quad (9)$$

The calculated values of q were found to be agree to within an average of 5.5 percent of measured values. The details of this analysis are contained in Appendix 3.

For the nonisothermal case, the measured results are illustrated in Fig. 17 and the calculated values in Fig. 18. Each line represents a constant temperature in chamber 1. The test conditions such as flow rate and insulation thickness were the same as the isothermal test. The ambient temperature, however, varied more widely, from 19°C to 24°C, than in the isothermal tests. The ambient temperature differences prevented the data points for each chamber temperature in Fig. 17 from

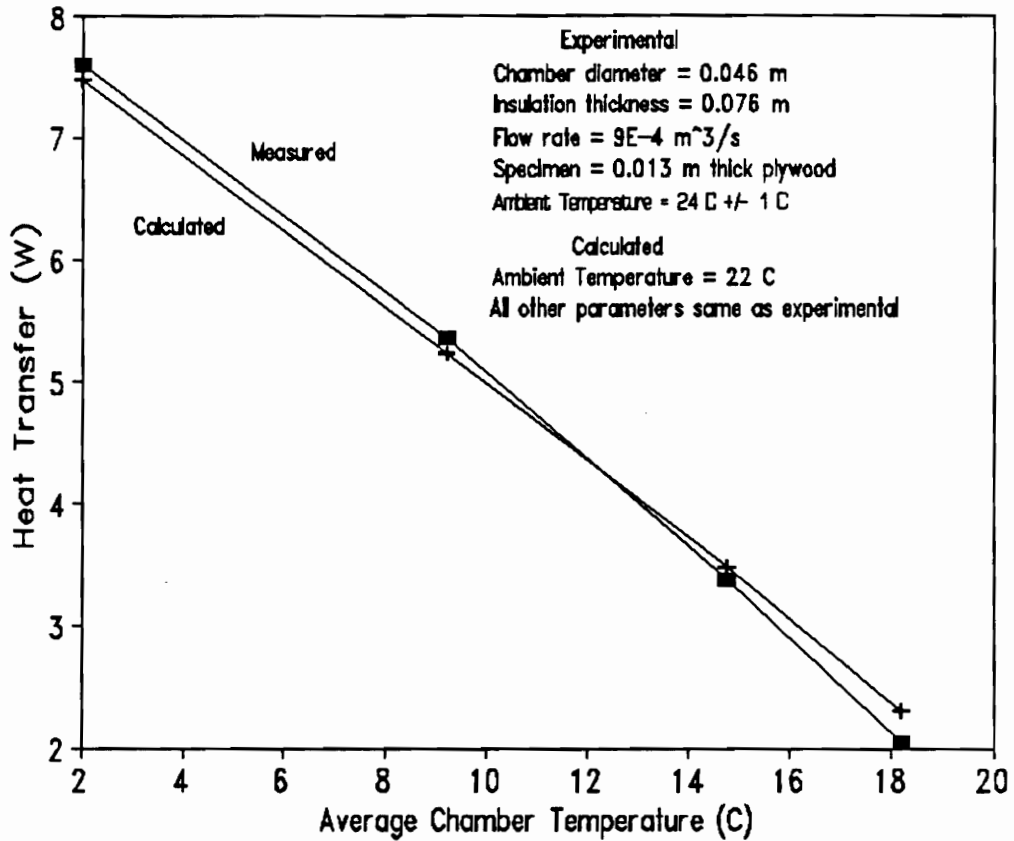


Fig. 16 Comparison of measured and calculated heat transfer for the isothermal case.

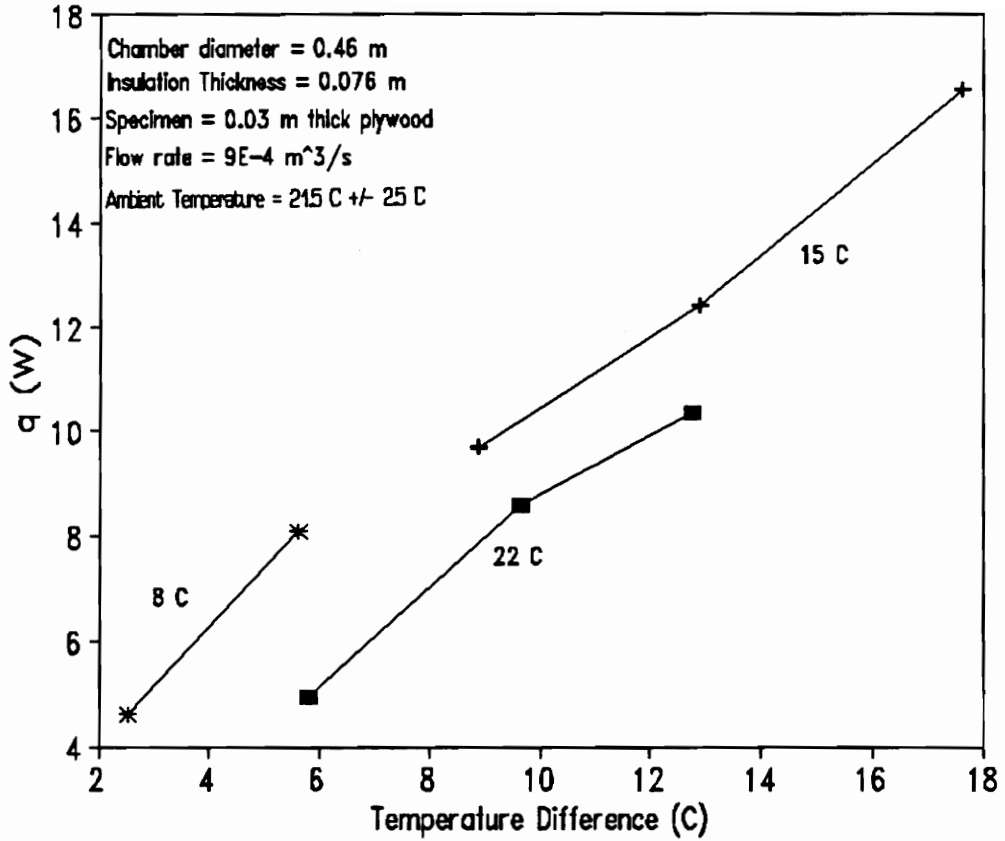


Fig. 17 Measured heat transfer vs temperature difference across specimen.

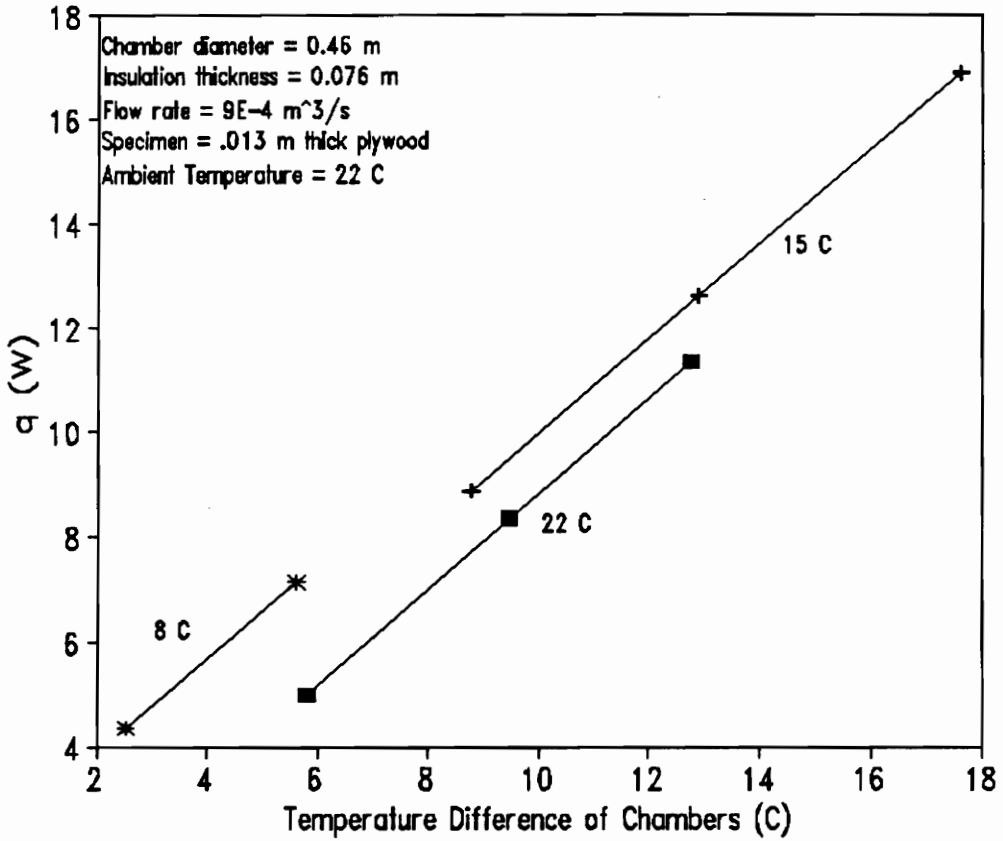


Fig. 18 Calculated heat transfer vs temperature difference across the specimen.

falling on a straight line. The measured chamber temperatures were used with a constant ambient temperature in the model to prepare Fig. 18. Figure 18 is essentially the calculated heat transfer for the chamber using the measured chamber temperatures and corrected for ambient temperature variation.

It will be shown later that the heat transfer through the specimen seriously limits the relative humidity operating range of the apparatus. To separate the total chamber heat transfer into the heat transfer through the specimen and the heat transfer from the ambient through the chamber wall, hereafter referred to as the "parasitic load", the data from the isothermal test were taken and heat transfer was divided in half. The resulting heat transfer is plotted on Fig. 19 as the parasitic load. In the isothermal test, the only heat transfer was parasitic so it is assumed that half of the total heat transfer can be attributed to each chamber.

To calculate the parasitic load, the first term on the right hand side of Eq. 9 was compared to the data. The results of this equation constitutes the second curve on Fig. 19. The difference between the measured and calculated values of the heat transfer is an average of 4 percent.

The combination of the parasitic load estimation and nonisothermal test results show how much the specimen contributes to the total heat transfer into or out of the chamber. As an example, with an ambient temperature of 21°C, if chamber 1 has a temperature of 15°C and chamber 2 has a temperature of 25°C, the parasitic effect on chamber 1 is approximately 1.5-1.7 W while the total heat transfer is

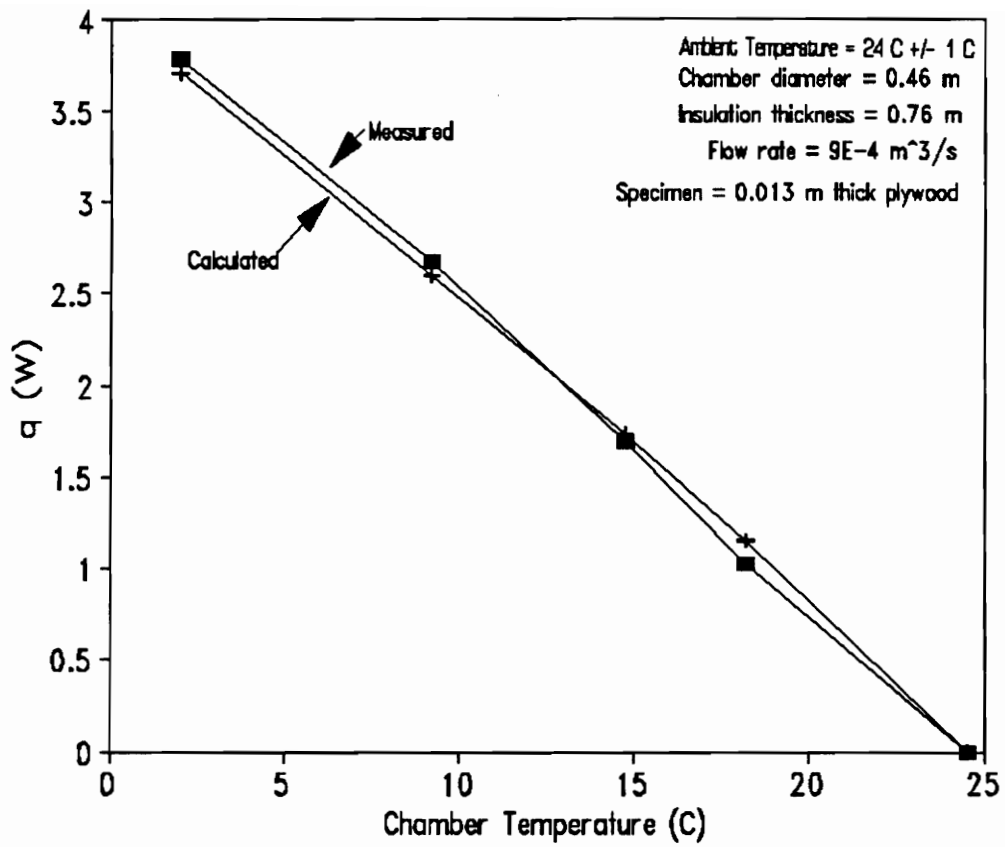


Fig. 19 Comparison of measured and calculated parasitic heat loss vs temperature difference across specimen.

approximately 10 W.

3.2.1 Spatial Temperature Variations Within the Chamber

Spatial temperature variation was measured within the chambers. To perform the test, a sheathed thermocouple was placed into the thermocouple fittings in the endplate of chamber 1 as shown in Fig. 20. The thermocouple was bent at an angle such that it could be turned to a different position in the chamber. The data were taken at points 0.03 m and 0.06 m from the specimen surface. The results of the tests are shown in Figs. 21 and 22 which also show the measurement locations. The temperature readings were taken in two different planes to verify that there is less variation at points nearer to the specimen surface.

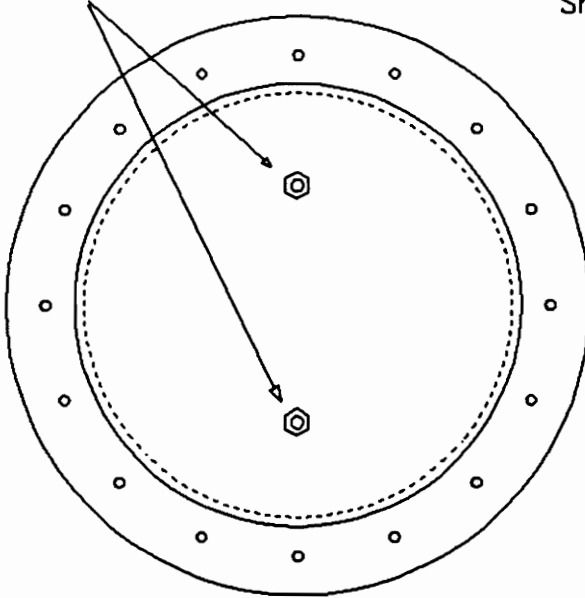
Temperature variation within the chamber, close to the specimen surface, is generally less than $\pm 1^\circ\text{C}$.

3.2.2 Time Varying Chamber Temperatures

The moisture transfer rate for porous materials is temperature dependent, so it is important to maintain a constant temperature within the chamber during operation. The ability to maintain a constant chamber temperature over time was investigated by controlling the temperature in chamber 1 to a desired setpoint, and measuring the temperature fluctuations in chamber 1, chamber 2, and the ambient air. The ambient temperature was manually manipulated to get a wide temperature variation.

The graphical results of the chamber temperature fluctuations is shown in

Thermocouple Fittings



Shielded Thermocouple

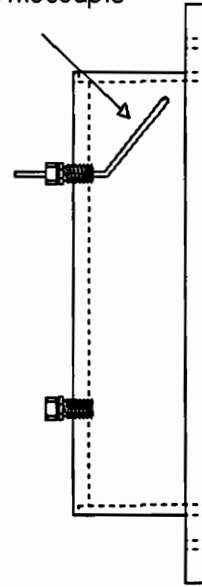


Fig. 20 Spatial temperature variation testing setup.

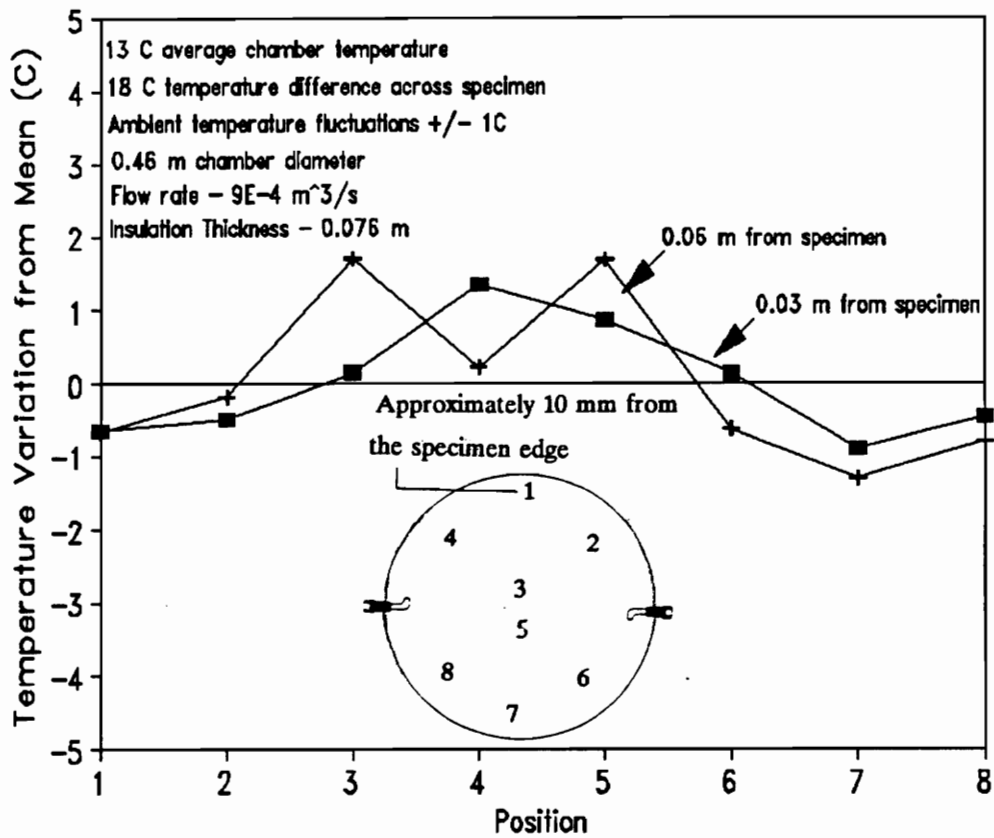


Fig. 21 Spatial temperature variation in chamber with 13°C chamber temperature and 18°C temperature difference across specimen.

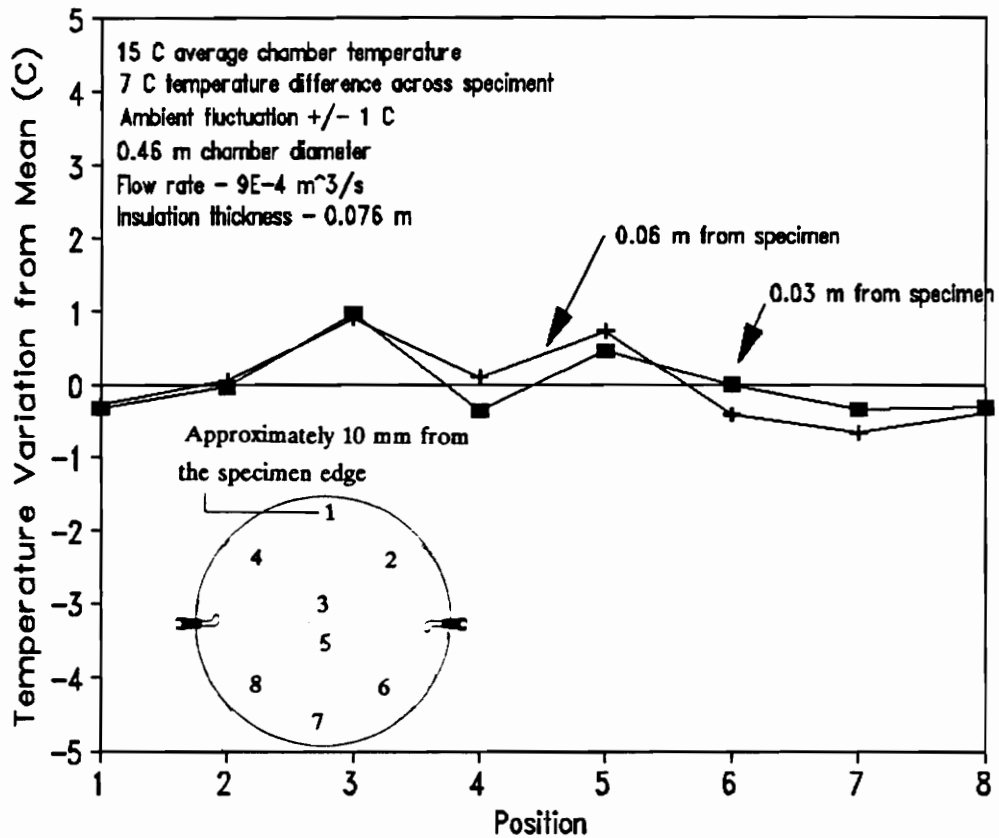


Fig. 22 Spatial temperature variation in chamber for a 15°C chamber temperature and a 7°C temperature difference across specimen.

Fig. 23. The test was run for 20 hours. The ambient temperature and a point in each chamber was measured every 5 minutes. Chamber 1 had a constant temperature to within $\pm 0.25^{\circ}\text{C}$. This degree of temperature control is within the original target limit.

Normal operation will always include an automatically controlled resistance heater in chamber 2. Only one automatically controlled resistance heater was available when the test was run, so the temperature of chamber 2 was controlled by the heat exchanger only. This fact accounts for the greater temperature variation in the temperature of chamber 2.

During normal operation, temperature fluctuations in both chambers is expected to be less than in this test. Having chamber 2 controlled only with the heat exchanger was a benefit because it was conservative. Chamber temperature variations in chamber 2 contribute more the temperature variations in chamber 1 than ambient temperature variations because of the higher heat transfer through the specimen.

3.3 Relative Humidity Control

Preliminary tests were conducted on the relative humidity control system in which automated control was disabled and the flow through the bubble and desiccant column was regulated by manually turning the valves. The purpose of manual control was to give an indication of how difficult relative humidity control would be. The dewpoint temperature was controlled manually to within $\pm 0.15^{\circ}\text{C}$ of a desired

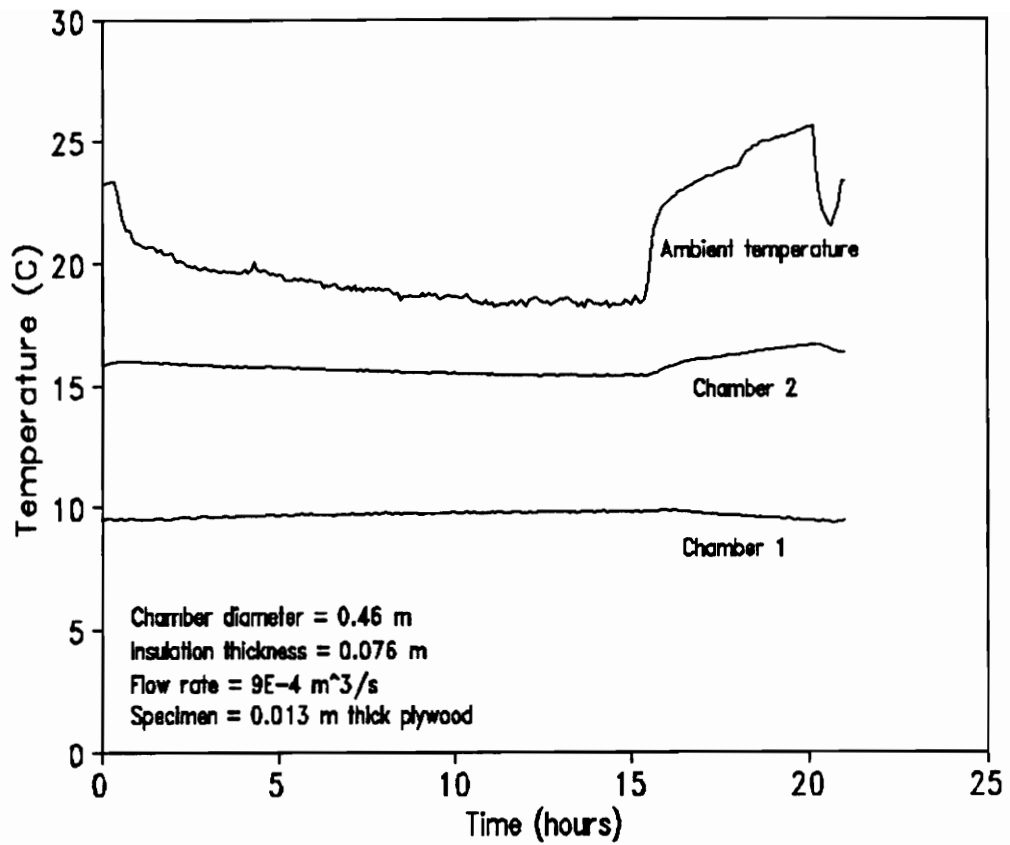


Fig. 23 Time varying temperature fluctuations within the chamber.

setpoint. A 0.15°C dewpoint temperature variation represents less than $\pm .75$ percent relative humidity variation across the target temperature range of the apparatus.

The automated control system was then enabled and the dewpoint was maintained to within approximately $\pm 0.25^\circ\text{C}$, which represents less than ± 1 percent variation in relative humidity.

3.4 Limits of Operation

The operating limits of the apparatus consists of both temperature limits and relative humidity limits.

3.4.1 Temperature limits

The temperature control system has the ability to maintain any temperature in the chamber from 5 to 60°C with a 20°C temperature difference across the specimen.

3.4.2 Relative Humidity Limits

The maximum relative humidity, for any given set of operating parameters (recirculating air flow rate, chamber temperature, insulation thickness, etc.) is fixed by the coldest spot on the air-side surface of the apparatus. Specifically, the dewpoint temperature of the air stream must be less than the temperature of the coldest spot. Otherwise, condensation occurs which is unacceptable.

For chamber temperatures lower than ambient temperature, the coldest spot in the system is the heat exchanger air-side wall surface because the heat exchanger cools the air to compensate for heat transfer into the chamber. More specifically,

the air-side wall temperature located at the coolant inlet will be the coldest spot in the heat exchanger and thus the coldest spot in the system. Conservatively, the heat exchanger air-side wall surface temperature is assumed equal to the coolant inlet temperature.

For chamber temperatures higher than ambient temperature, the coldest spot in the apparatus is the pipe (tubing) wall at the pump inlet. The piping is cooled by ambient air. The pump heats the air as it flows through.

3.4.2.1 Chamber Temperatures Lower Than Ambient Temperature

The relative humidity limits for chamber temperatures lower than ambient temperature are shown in Fig. 24. To determine these limits, it is necessary to determine the air outlet surface temperature of the heat exchanger (or the coolant inlet temperature) for any set of operating parameters. This temperature can be determined from the following procedure:

1. Determine the total heat transfer into the chamber from Fig. 18 or Eq. 9.
2. Calculate the chamber inlet to outlet temperature difference from Eq. 6 using the result from step 1.
3. Estimate the inlet chamber temperature by subtracting the temperature difference found in step 2 from the average chamber temperature (assumed to be the outlet temperature).
4. Calculate the required heat exchanger air outlet temperature from an energy balance on the piping between the heat exchanger and the chamber inlet.

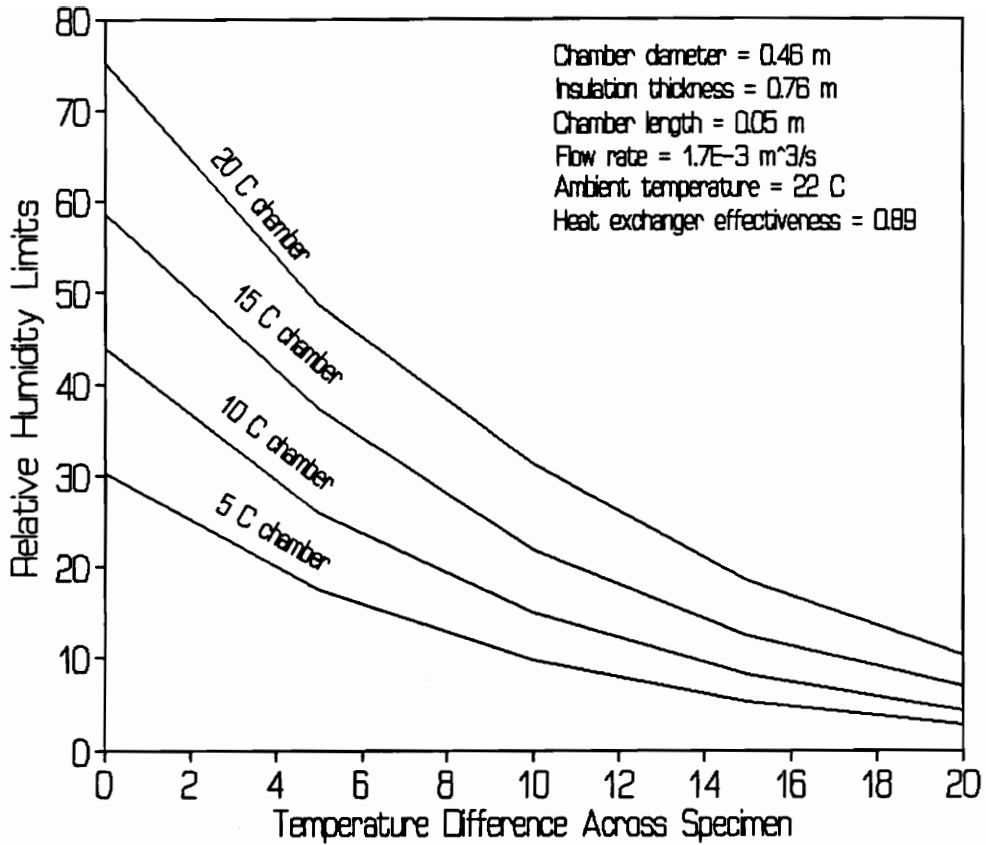


Fig. 24 Relative humidity limits for the present apparatus when the chamber is operating at temperatures lower than ambient temperature.

This result is returned to in step 8.

- Using a measured or calculated UA for the heat exchanger calculate the NTU where

$$NTU = \frac{UA}{C_a} \quad (10)$$

- Determine the counter-flow heat exchanger effectiveness from

$$\epsilon = \frac{1 - \exp[-NTU(1 - C_r)]}{1 - C_r \exp[-NTU(1 - C_r)]} \quad (11)$$

- The coolant inlet temperature is then be determined from

$$\epsilon = \frac{T_{a,i} - T_{a,o}}{T_{a,i} - T_{f,i}} \quad (12)$$

- At least 2°C must be subtracted from the result of step 9 because the controller varies the input temperature to maintain a particular chamber temperature in response to a temperature disturbance, such as a fluctuating ambient temperature.

Calculating the chamber inlet temperature using step 3 is a conservative approach. The average chamber temperature actually falls between the temperature of the inlet and the outlet of the chamber, but exactly where is difficult to determine. Experimentally the average chamber temperature was found to fall somewhere between 1 to 20 percent of the total inlet to outlet temperature difference less than the outlet temperature. For example, if the chamber had an inlet to outlet

temperature difference of 10°C, the average chamber temperature would be from 0.1 to 2°C below the temperature of the outlet air. The difference between the average chamber temperature and the outlet will vary with the average chamber temperature and the temperature difference across the specimen.

The energy balance in step 4 is accomplished using

$$(UA)_p [T_a - T(x)] = \dot{m}_a (h_{a,i} - h_{a,o})_p \quad (13)$$

Substituting $C_p dT$ for h , $d_i \pi(dx)$ for A , and integrating between the outlet of the heat exchanger and the chamber inlet results in

$$(T_{a,i})_p = T_a - e^{\left[\frac{\pi U d_i}{(\dot{m} C_p)_a} \right]} (T_a - T_{c,i}) \quad (14)$$

Experimentally, the air temperature entering the heat exchanger was observed to be approximately 27°C irrespective of the operating conditions. The pumps heat the air as the air passes through before entering the heat exchanger.

3.4.2.2 Chamber Temperatures Higher Than Ambient Temperature

The limits of operation for chamber temperatures higher than ambient are shown in Fig. 25. To calculate these limits it is necessary to determine the temperature of the piping wall surface temperature at the air inlet to the pump. The procedure for determining this temperature, assuming the wall surface temperature is equal to the air stream temperature, is as follows:

1. Determine the total heat transfer into the chamber from Fig. 18 or Eq. 9.

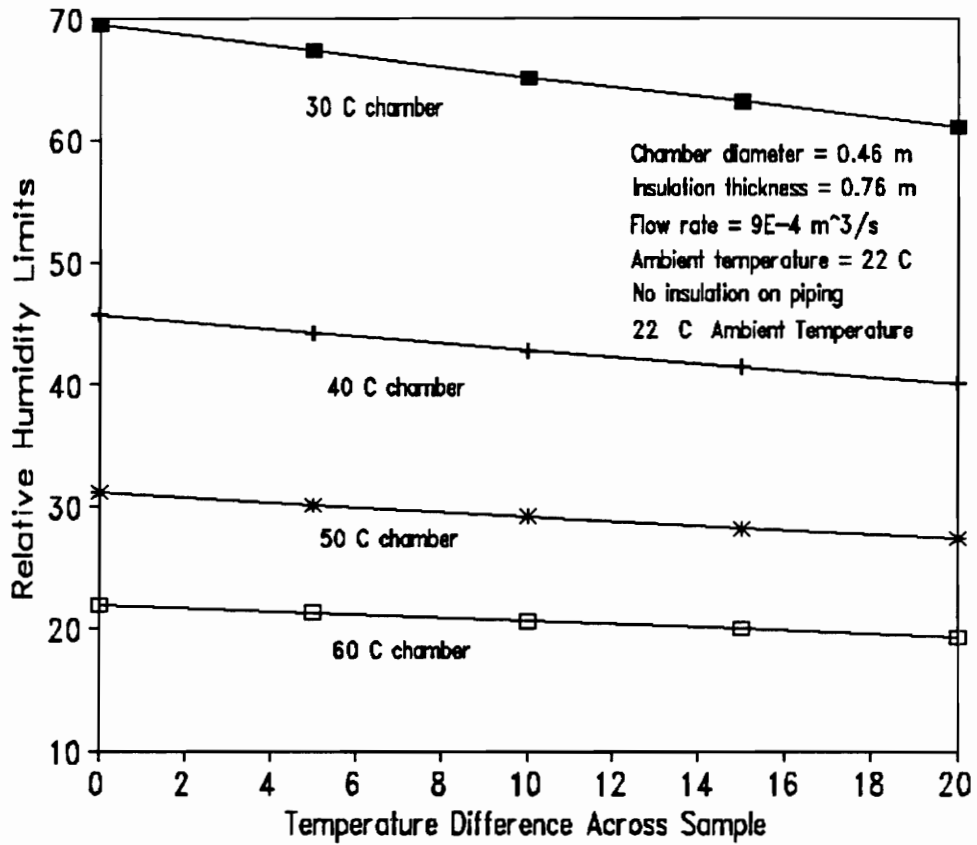


Fig. 25 Relative humidity limits of the apparatus when the chamber is operating at temperatures higher than ambient temperature.

2. Calculate the chamber inlet to outlet temperature difference from Eq. 6.
3. Estimate the outlet chamber temperature by adding the temperature difference found in step 2 to the average chamber temperature. The average chamber temperature is assumed to be equal to the inlet temperature for a conservative estimate of the outlet temperature.
4. Calculate the heat exchanger air outlet temperature from an energy balance on the piping between the chamber and the pump inlet.

Achieving high relative humidities at high temperatures is also a challenge. Preliminary tests showed that as air is bubbled through the bubble column it is humidified to a dewpoint of approximately 1°C less than the water temperature. This observation means that the bubble column will require heating.

3.5 Leak Tests

It was necessary to check the air circulation systems for leaks because any leaks would result in serious error in the data. Leak tests were conducted by applying a static pressure to a portion of the system, and periodically checking for a pressure drop on a pressure gauge or manometer.

Preliminary runs showed that the leakage rates in the diaphragm pumps were much higher than expected. Consequently, the sources and significance of pump leakage was examined. The pumps were checked with a dynamic test in addition to the static test to determine if movement between the diaphragm and the diaphragm housing was causing leaks. Static tests would not indicate this type of leak.

Dynamic tests were performed by placing the pump in series with a desiccant column and a dewpoint hygrometer in parallel as shown in Fig. 26. The air was allowed to circulate through the desiccant for a period of time. When the air was sufficiently dry, the desiccant column was closed off and the change in the dewpoint was observed. From this data, using an approximation of the ambient temperature, ambient relative humidity, and volume of the system, an estimation of volume leak rate was calculated.

It was found that the error contributed by these pumps to the moisture diffusion data for highly permeable materials would be negligible. However, for the less permeable materials, the error could be significant. Under relatively dry conditions (5 to 10°C and 30 to 50 percent relative humidity) an error of approximately 2.5 percent of the measured weight difference in the desiccant or bubble column could be contributed by leakage in the pumps. When the ambient temperature and relative humidity are higher (22°C and 30 to 60 percent relative humidity) the error could reach 11 percent.

The pump tests were performed mainly in the lower dewpoint starting ranges (-40°C to -50°C) because, as indicated with the flatness of the psychometric chart curve in this region, a smaller amount of moisture will yield a greater change in dewpoint for a given time period. Time data over the range of a 20°C to 30°C dewpoint temperature rise was recorded and averaged. A static test of approximately 380 kpa (40 psig) assured that the piping and dewpoint hygrometer were airtightness.

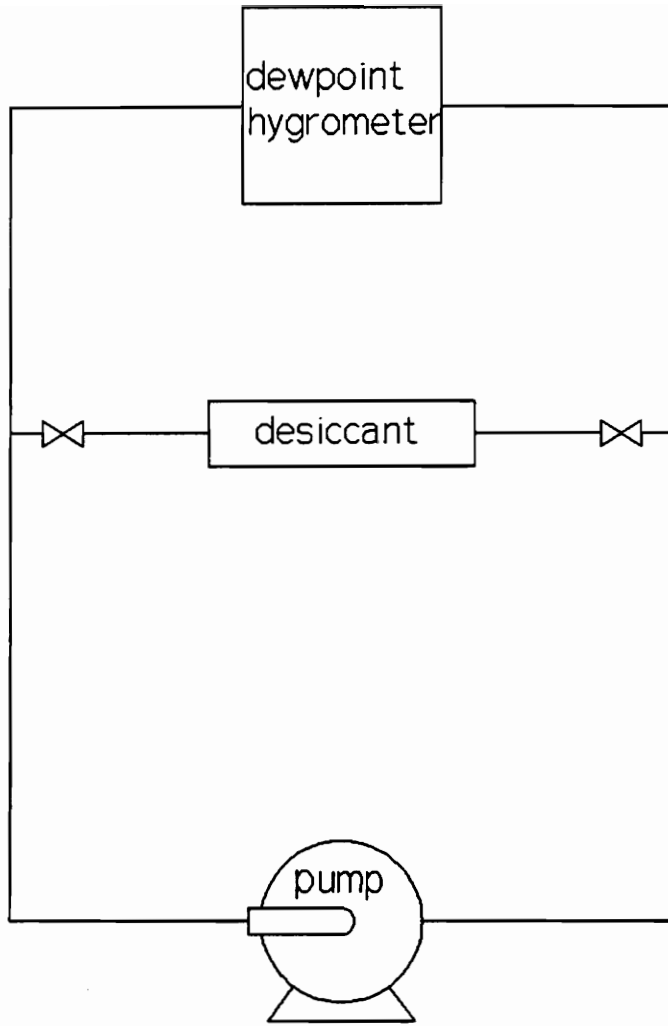


Fig. 26 Dynamic pump leak test setup

IV. Discussion and Recommendations

The improvements that could be made in the apparatus to increase the relative humidity operating range and to improve temperature and relative humidity control are discussed in this section. Changes that could be made to the chamber and the circulation system are also discussed.

4.1 Increasing the Relative Humidity Operating Range

The methods to increase the operating ranges for chamber temperatures lower than ambient temperature will be discussed first. The methods to increase the operating ranges for chamber temperature higher than ambient temperature will follow.

4.1.1 Chamber Temperatures Lower Than Ambient Temperature

The upper relative humidity operating limit when operating at temperatures lower than ambient temperature can be increased by a) increasing the recirculating air flow rates and b) reducing the heat gains to the chamber and connecting piping to the heat exchanger. The piping gains can be reduced, of course, by reconfiguring the piping to make it shorter and by increasing the insulation thickness. Reducing the chamber gains can be accomplished by decreasing the size of the chamber, test specimen, and holder, and by increasing the insulation thickness.

4.1.1.1 Effect of Higher Recirculating Air Flow Rates

Raising the flow rate is an effective way to increase the relative humidity upper limits, as shown in Fig. 27. Equation 8 shows that $(T_{out}-T_{in})$ decreases as the

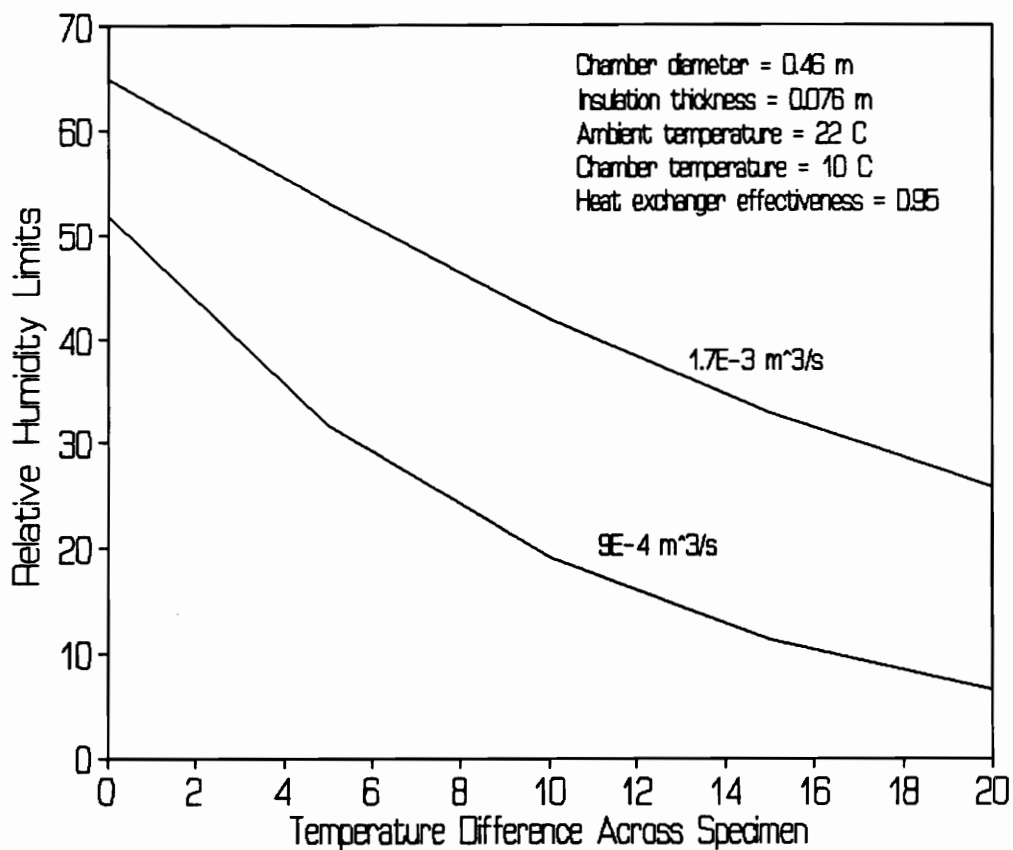


Fig. 27 Differences in the operating limits for different flow rates vs temperature difference across the specimen.

mass flow rate increases, for the same heat gain. With a smaller temperature difference between the inlet and outlet of the chamber, the heat exchanger air outlet temperature can be higher, thus increasing the maximum allowable dewpoint temperature.

4.1.1.2 Effect of Decreasing the Chamber Size

Decreasing the chamber diameter is another way to increase the operating range. A smaller chamber diameter reduces the heat transfer across the specimen and holder, thus increasing the minimum air supply temperature. The effect of decreasing the chamber size on the operating range is shown in Fig. 28. The trade-off is the reduced moisture transfer rate with the smaller specimen area. Figures 29 and 30 compare the effect of chamber diameter on total diffusion by showing the time to achieve a least count maximum uncertainty of 5 percent (0.02 g moisture). A 0.305 m (12 in.) chamber diameter is a good compromise for materials with diffusivity characteristics as low as white pine, considering the number of weight measurements desirable per week (2 or 3).

4.1.1.3 Effects of Other Methods

Reducing the chamber length and increasing the insulation thickness around the chamber will each contribute a relatively small benefit to the operating ranges. Reducing the chamber length would lessen the parasitic load and could be applied to the present chamber without sacrificing total moisture diffusion. Based on experience, decreasing the length of the present chamber by half would allow enough

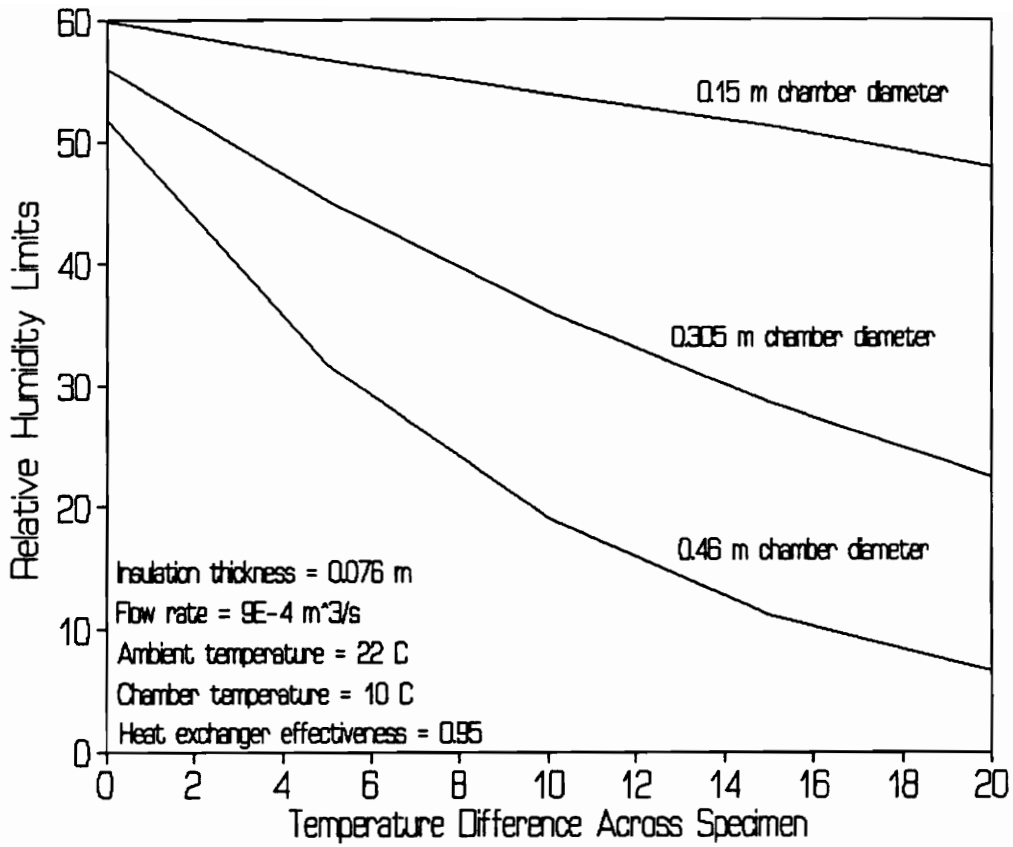


Fig. 28 Differences in the operating limits for various chamber diameters vs temperature differences across the specimen.

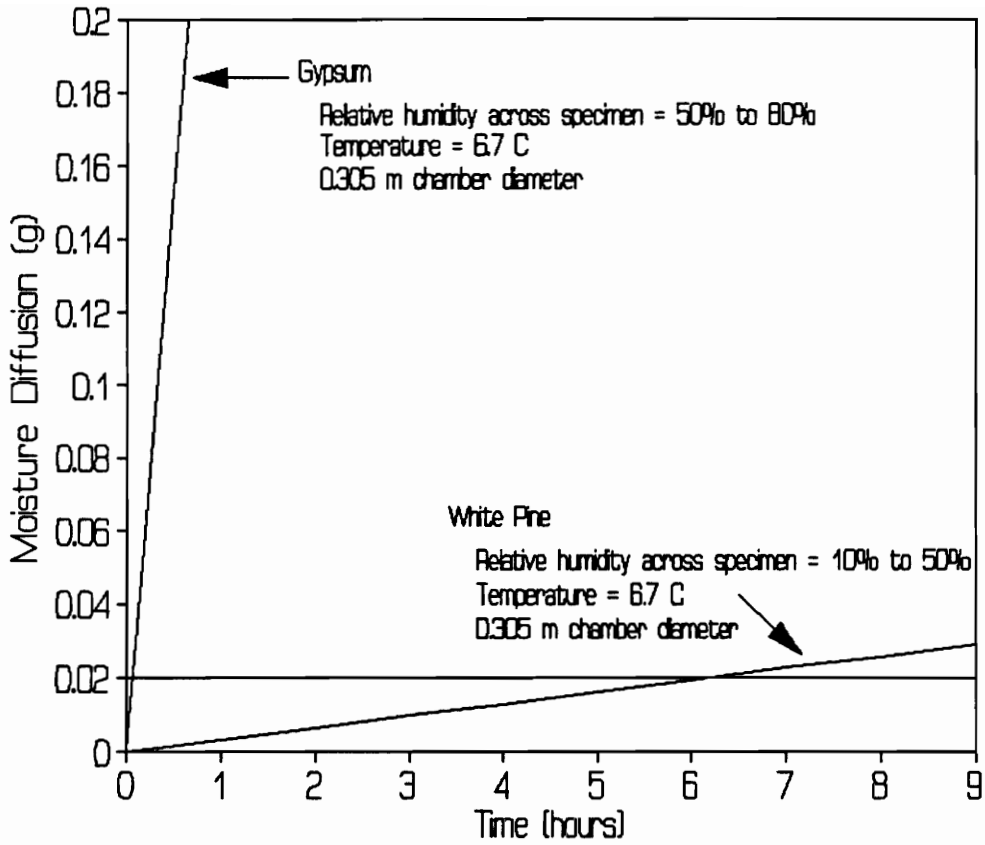


Fig. 29 Total moisture transfer vs time for a chamber diameter of 0.305 m.

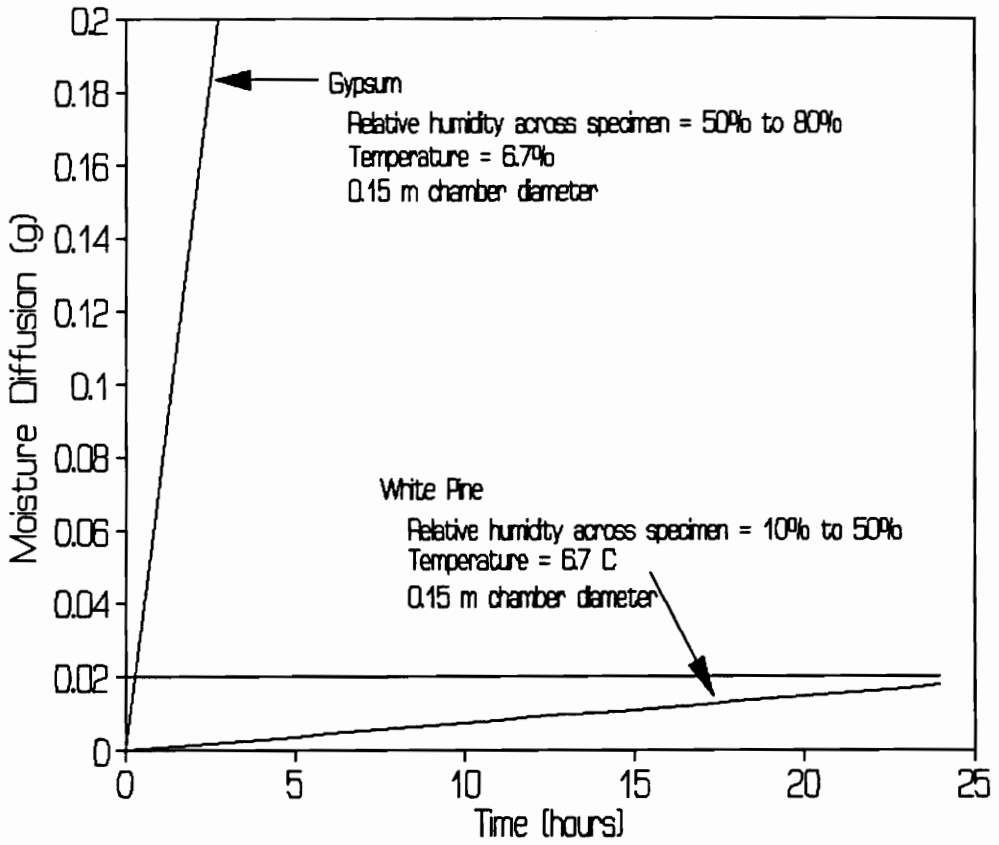


Fig. 30 Total moisture transfer vs time for a chamber diameter of .15 m.

room for mixing and installing the fittings in the chamber wall. Increasing the insulation thickness would, like shortening the chamber length, lessen the parasitic load on the chambers. The effect of increasing the insulation thickness on the chambers is shown in Fig. 31.

4.1.1.4 Recommendations

Based on the above analysis, it is recommended that for material specimens with diffusivities as low as for white pine, the chamber diameter be reduced from 0.46 m (18 in.) to 0.305 m (12 in.), the flow rate be increased from $9.2 \times 10^{-4} \text{ m}^3/\text{s}$ to $1.7 \times 10^{-3} \text{ m}^3/\text{s}$, and the chamber length be shortened from .1 m (4 in.) to .05 m (2 in.). Considering these changes in the present system, the resulting operating ranges for chamber temperatures lower than ambient temperature are shown in Fig. 32. The piping between the heat exchanger and the chamber has also been shortened in the analysis. The increases in relative humidity limits are 5 to 10 fold at the extreme temperature difference of 20°C across the specimen.

4.1.1.5 Effect of the Heat Exchanger on the Operating Limits

In the previous analysis of increasing the operating range, the heat exchanger was assumed to have an effectiveness of 0.95, as stated in the figures, rather than 0.885 (stated in Fig. 24) as with the present heat exchanger. Increasing the effectiveness in the analysis is based on the assumption that the heat exchanger has been redesigned to decrease the temperature difference between the air outlet of the heat exchanger and the inlet of the heat exchanger cooling fluid. For an ideal

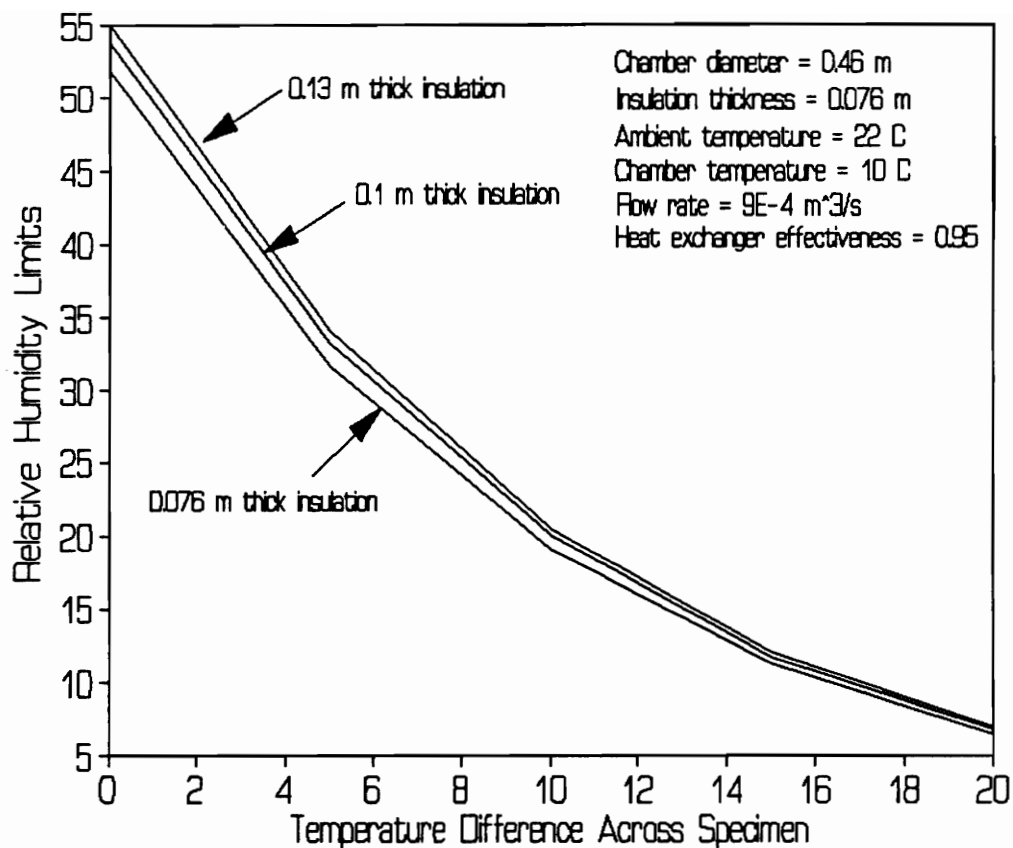


Fig. 31 Differences in the operating limits for various insulation thicknesses vs temperature differences across the specimen.

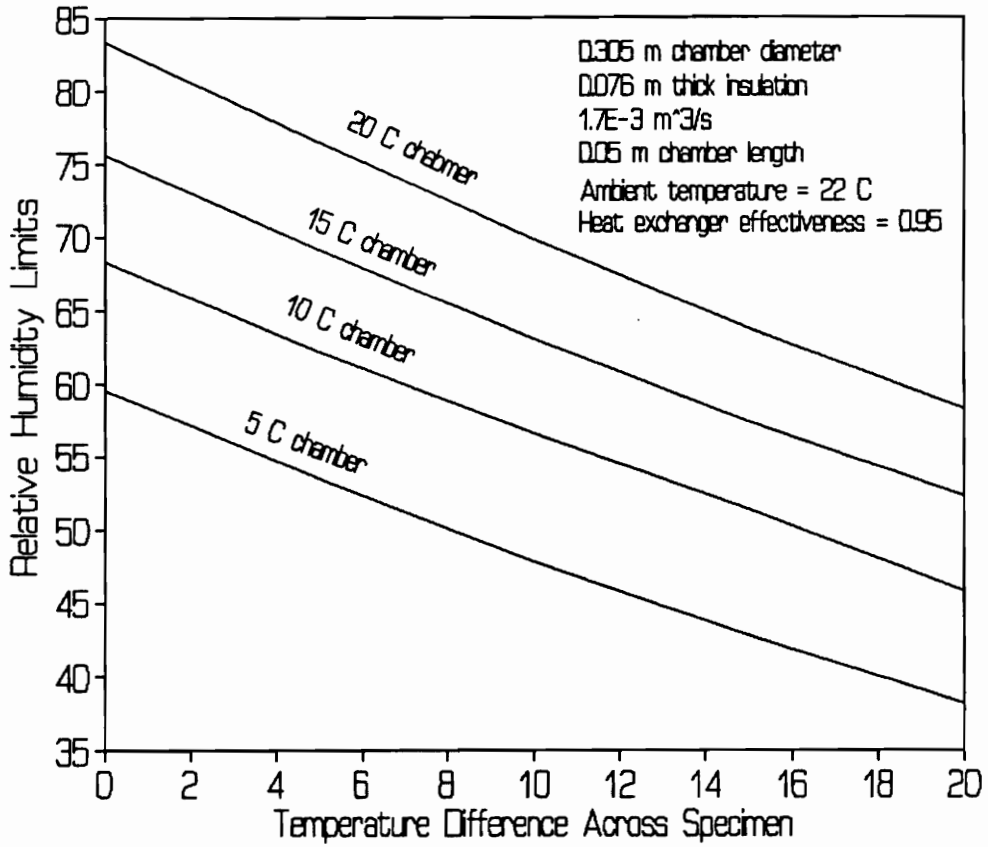


Fig. 32 Operating limits with 0.305 chamber diameter, 0.05 chamber length, $1.7 \times 10^{-3} \text{ m}^3/\text{s}$ flow rate, 0.076 m thick insulation.

effectiveness of 1.0, the coolant inlet temperature would be the same as the outlet air temperature. To approach this ideal, it would be better to redesign the heat exchanger rather than to simply enlarge it. For example, a finned air-side would effectively increase the surface conductance between the heat exchanger and the air stream and make the heat exchanger more effective.

4.1.2 Chamber Temperatures Higher Than Ambient Temperature

The relative humidity ranges for operating temperatures higher than ambient temperature can be increased by insulating the piping. Applying 0.032 m-thick (1.25 in.) insulation to the entire piping system increases the relative humidity operating range to that shown in Fig 33.

4.3 Relative Humidity Control

Proportional-integral-differential (PID) control with the control parameters set for a heavily dampened response should be used to control the relative humidity. Proportional-integral control is complicated by a slow diffusion process. The reason is that a proportional-integral normal control response includes oscillation around the setpoint. With a well sealed chamber, the ways to eliminate moisture in the chambers are diffusion through the specimen and desiccant absorptance. Moisture diffusion is a slow process, so if the setpoint is overshoot, the time for the dewpoint temperature to return to or fall below the setpoint as a result of moisture transfer through the specimen would be prohibitive on any kind of normal control. If the desiccant column is used in addition to the bubble column for moisture control in the

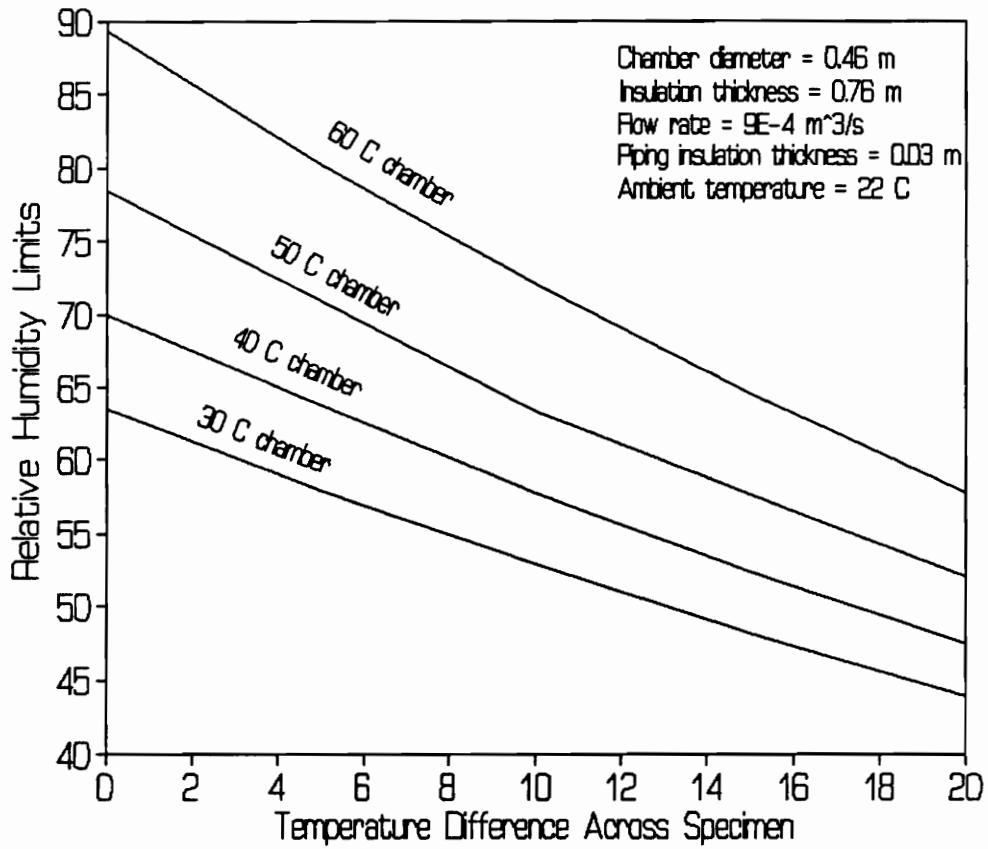


Fig. 33 Relative humidity limits when insulation is applied to the piping between the chamber and the pump for chamber temperatures higher than ambient.

same chamber, the bubble and desiccant columns on each side of the specimen would need to be weighed to determine moisture transfer. Weighing all four columns increases the least count uncertainty. The possibility also exist of saturating the desiccant column before adequate moisture has been transferred through the specimen for an accurate measurement. The degree of control achieved in the relative humidity automated control tests was actually facilitated by leaks that were in the chamber. During normal operation, leaks would be sealed which would make control more difficult. A separate control algorithm could also be written that takes the unique response of this system into account.

Regardless of the algorithm used, the relative humidity control is expected to improve with higher recirculating air flow rates. A contributing factor to the response lag is the length of piping between the desiccant and bubble columns, and the chamber. As the velocity of the air stream increases, the response lag should decrease, making control easier.

4.4 Pumps

Since leakage in the pumps causes significant error in moisture transfer data, an investigation was performed to determine the best pumps for this application. Peristaltic pumps, diaphragm pumps, and bellows assembly pumps were considered. The pumps recommended for this application are metal bellows pumps. Metal bellows pumps produce high flow rates and are highly leak tight. The specific pump recommended is the Parker Metal BellowsTM model MB-602. This pump produces

$2.8 \times 10^{-3} \text{ m}^3/\text{s}$ at free flow. The leak tightness is $1 \times 10^{-4} \text{ cc}_{\text{He}}/\text{s}$ in the standard configuration and can be improved to $1 \times 10^{-7} \text{ cc}_{\text{He}}/\text{s}$ with a leak reduction option. The values on leak tightness are measured by the pump manufacturer by placing a 1 atmosphere pressure difference between the inside and the outside of the pump, and placing the pump into a helium environment.

To provide an indication of whether the pump was sufficiently airtight, it was assumed that when the pump is running, air will leak at the same rate as helium in the helium static leak test. With ambient conditions of 21°C and 65 percent relative humidity, and using white pine as the specimen material with the worst case diffusion rate from Table 1, pump leakage would contribute 0.06 percent error to the weight change measurements of the desiccant and bubble columns. The leak reduction option would decrease the calculated error to 6×10^{-5} percent. If the leak is 100 times worse than calculated, the pump is still sufficiently airtight with the leak reduction option.

4.5 Use of Acrylic

The acrylic chamber and bubble columns are the most troublesome parts of the apparatus to seal. Acrylic is brittle and when used in thin sections, such as in portions of the bubble column, it tends to crack when assembled. Also, when connecting and disconnecting the piping to the column, leaks tend to form between the fittings and the acrylic wall.

The joint where the flange contacts the chamber wall is also difficult to seal.

The solvent cement itself seals well, but it is hard to cover the entire area to be sealed. The voids in the joint act as cracks. As the apparatus is assembled, the bolts place a moment on the joint which causes a stress concentration at the tip of the cracks. The stress concentration tends to fracture the bonded part of the joint to relieve the stresses. The flanges break completely free of the chamber wall in places around the circumference or at least have small leaks. As this material will be used in the future during actual diffusion tests, extreme care will need to be taken to assure that the system is leak tight. The flange could be reinforced by a rigid, metal ring which would more evenly distribute the load of the bolts. The chamber itself may need to be redesigned in some way to alleviate this problem.

The piping system is simple to seal except where the fittings are threaded into the acrylic chambers. Leaks can be corrected by further tightening the fittings into the chamber wall, but this tends to craze the material radially around the tapped hole.

V. Conclusions

A workable design for measuring the moisture transfer in porous materials has been developed which fulfills the original objectives. The apparatus has the ability to control the moisture content of the recirculating air, and thus the relative humidity in the chamber, without the use of saturated salt solutions. Chamber temperatures of 5°C to 60° can be maintained with a temperature difference across the specimen up to 20°C.

The operating ranges, based on the air outlet temperature, for the present apparatus are for the isothermal case 21 percent relative humidity for a 60°C chamber temperature to 52 percent relative humidity for a 5°C chamber temperature. For the nonisothermal case with a 20°C temperature difference across the specimen the operating ranges are a 16.3 percent relative humidity for a chamber temperature of 60°C chamber temperature, and 7.2 percent relative humidity for a 5°C chamber temperature. The relative humidity operating range increases to 75 to 85 percent as the chamber temperatures approach the ambient temperature. These limits assume a 22°C ambient temperature. The relative humidities increase as the chamber temperature approaches the ambient temperature.

Diffusion will be high enough with the present apparatus to obtain accurate measurements, given the resolution of the scale, within a reasonable amount of time (2 or 3 measurements per week) for materials that have diffusivity characteristics at least as low as white pine after steady state moisture transfer conditions have been

reached.

The specimen load is the most important heat transfer effect under nonisothermal test conditions.

The temperature controller controls the chamber temperature to $\pm 0.4^{\circ}\text{C}$.

Temperature variation within the chamber, close to the specimen surface, is generally less than $\pm 1^{\circ}\text{C}$.

The relative humidity control can be manually controlled to $\pm 0.15^{\circ}\text{C}$ of the desired dewpoint. Using automated control, the relative humidity was controlled to within approximately $\pm 0.25^{\circ}\text{C}$ which is within ± 1 percent relative humidity. The degree of control, however, was likely improved by leaks in the system.

References

ASTM 1988, "Standard Test Methods for Water Vapor Transmission of Materials," *Annual Book of ASTM Standards*, ASTM E96-80, pp. 855-864.

Douglas, S.D., 1991, "Determination of Moisture Transport Properties for Common Building Materials: Method and Measurements," University of Minnesota, pp. 1-46.

TenWolde, A., 1989, "Moisture Transfer Through Materials and Systems in Buildings," *Water Vapor Transmission Through Building Materials and Systems: Mechanisms and Measurement*, ASTM STP 1039, H.R. Trechsel and M. Bomberg, Eds., American Society for Testing and Materials, Philadelphia, pp. 11-18.

Fanney, A.H., Thomas, W.C., Burch, D.M., and Mathena, L.R.Jr., 1991, "Measurements of Moisture Diffusion in Building Materials," *ASHRAE Transactions*, Vol. 97, Part 2, pp. 99-113.

Incropera, F.P. and De Witt, D.P., 1985 *Fundamentals of Heat and Mass Transfer*, 2nd ed., John Wiley and Sons, pp. 282-285, 502-538.

Sterling, E. M., Arundel, A., and Sterling, T.D., 1985, "Criteria for Human Exposure to Humidity in Occupied Buildings," *ASHRAE Transactions*, Vol. 91, Part 1B, pp. 611-622.

Thomas, W.C., and Burch, D.M., 1990, "Experimental Validation of a Mathematical Model For Predicting Water Vapor Sorption at Interior Building Surfaces," *ASHRAE Transactions*, Vol. 96, Part. 1, pp. 487-496.

Tveit, A., 1966, "Measurements of Moisture Sorption and Moisture Permeability of Porous Materials," *Norwegian Building Research Institute, Report 45*, Oslo, Norway, pp. 1-39.

White, J.H., 1989, "Moisture Transport in Walls: Canadian Experience," *Water Vapor Transmission Through Building Materials and Systems: Mechanisms and Measurement*, ASTM STP 1039, H.R. Trechsel and M. Bomberg, Eds., American Society for Testing and Materials, Philadelphia, pp. 35-50.

Appendix 1 Moisture Diffusion Model

This section outlines the moisture diffusion model used to estimate the moisture transfer rate when designing the apparatus.

The moisture diffusion rate is calculated from the mathematical model developed by Thomas and Birch (1990)

$$\dot{m}'' = \frac{\gamma_{s1} - \gamma_{s2}}{\frac{L}{\rho_d \bar{D}}} \quad (15)$$

If the diffusion coefficient, D , is as chosen in the form

$$D = D_0 e^{a\gamma} \quad (16)$$

then for the resistance network shown in Fig. 34

$$\dot{m}'' = \frac{P_v(\gamma_1) - P_v(\gamma_2)}{R_{s1}} = \frac{D_v(\gamma_2) - D_v(\gamma_3)}{\frac{aL}{\rho_d}} = \frac{P_v(\gamma_3) - P_v(\gamma_4)}{R_{s3}} \quad (17)$$

For one side of the specimen, the mass flux through the air can be written (Incropera, et al., 1985)

$$\dot{m}'' = \frac{h_m P_g (\phi_1 - \phi_2)}{RT} = h_m (\rho_{v1} - \rho_{v2}) \quad (18)$$

So for the each leg of the network the mass flux can be written as

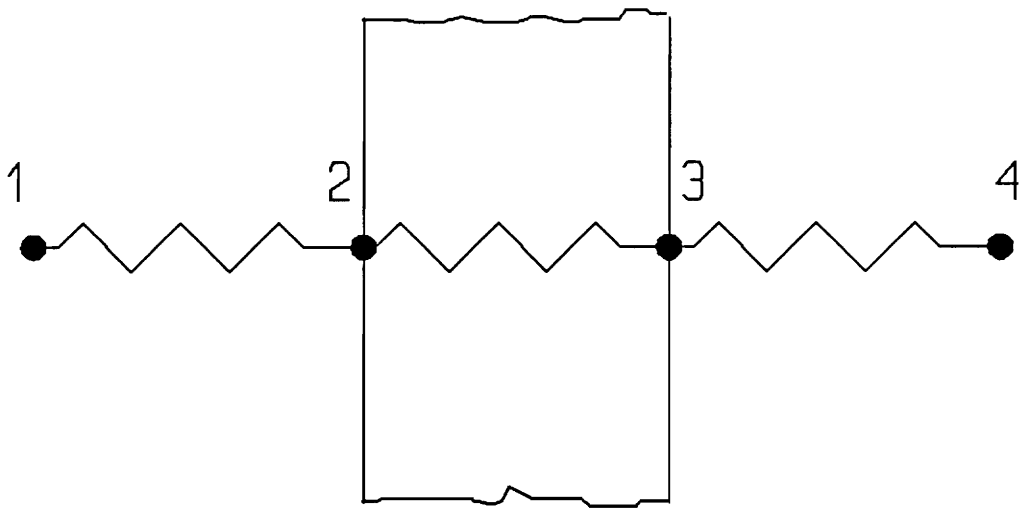


Fig. 34 Resistance network for mass diffusion through a specimen

$$\dot{n}'' = \frac{\gamma_1 - \gamma_2}{\frac{RT}{P_g h_m} \frac{\phi_1 - \phi_2}{\phi_1 - \phi_2}} = \frac{\gamma_2 - \gamma_3}{\frac{aL}{\rho_d} \frac{\gamma_2 - \gamma_3}{D_v(\gamma_2) - D_v(\gamma_3)}} = \frac{\gamma_3 - \gamma_4}{\frac{RT}{P_g h_m} \frac{\phi_3 - \phi_4}{\phi_3 - \phi_4}} \quad (19)$$

Equation 16 can also be written as

$$\dot{n}'' = \frac{\gamma_1 - \gamma_4}{\frac{RT}{P_g h_m} \frac{\gamma_1 - \gamma_2}{\phi_1 - \phi_2} + \frac{aL}{\rho_d D_o} \frac{\gamma_2 - \gamma_3}{e^{\alpha\gamma_2} - e^{\alpha\gamma_3}} + \frac{RT}{P_g h_m} \frac{\gamma_3 - \gamma_4}{\phi_3 - \phi_4}} \quad (20)$$

or

$$\dot{n}'' = \frac{D_v(\gamma_1) - D_v(\gamma_4)}{\frac{RT}{P_g h_m} \frac{D_v(\gamma_1) - D_v(\gamma_2)}{\phi_1 - \phi_2} + \frac{aL}{\rho_d} \frac{\gamma_2 - \gamma_3}{D_v(\gamma_2) - D_v(\gamma_3)} + \frac{RT}{P_g h_m} \frac{D_v(\gamma_3) - D_v(\gamma_4)}{\phi_3 - \phi_4}} \quad (21)$$

The convective mass transfer coefficient, h_m , is determined by (Incropera et al., 1985)

$$h_m = h \left(\frac{D_{AB} Le^{\frac{2}{3}}}{k} \right) \quad (22)$$

The vapor-in-air diffusion coefficient, D_{AB} , is obtained from Thomas and Birch (1990). The Lewis number is calculated from

$$Le = \frac{k}{\rho C_p D_{AB}} \quad (23)$$

To solve for the mass flux, an iterative approach is necessary because the

specimen moisture contents, γ , at the surfaces are unknown. After choosing a first guess, the new γ_2 and γ_3 are calculated from

$$\gamma_2 = \gamma_1 - n''R \quad (24)$$

and

$$\gamma_3 = \gamma_4 + n''R \quad (25)$$

Iteration is continued until the surface moisture contents stops changing.

Appendix 2 Molecular Sieve Tests

Test were conducted to help determine the proper size of desiccant columns necessary to absorb moisture for a reasonable length of time before the columns become saturated. The test were conducted by constructing columns of molecular sieve of three heights. The heights chosen were 0.14 m (5.5 in.), 0.28 m (11 in.), and 0.56 m (22 in.). Ambient air was pumped through the desiccant at 0.037 m/s (3 scfh/in²), 0.11 m/s (9scfh/in²), 0.44 m/s (18 scfh/in²), and 0.44 m/s (36 scfh/in²). The ambient air had a dewpoint of approximately 12°C.

The test velocities were chosen relative to the estimated moisture transfer into the chamber through the specimen. The procedure was as follows:

1. Estimate the amount of moisture transfer from the diffusion model in Appendix 2.
2. Calculate the humidity ratio of the chamber air from

$$\omega = .622 \frac{P_v}{P_a} \quad (26)$$

3. Calculate the mass flow rate from the resulting values of step 1 and 2 from

$$\dot{m} = \frac{\dot{r}}{\omega} \quad (27)$$

4. Calculate the volume flow rate from the ideal gas equation of state

$$\dot{V} = \dot{m} \frac{RT}{P} \quad (28)$$

5. The velocity can be determined by dividing by the cross-sectional area of the column.

This procedure assumes that the desiccant will completely dry the air.

The graphical results of the tests are shown in Figs. 35 to 38. In all but the highest flow rate, the desiccant columns generally maintain a constant dewpoint at the outlet until saturation, regardless of the column height.

The weight of desiccant to absorb 1 g of moisture, under the stated conditions of this test is given in Table 2. The amount of desiccant needed to dry a certain quantity of moisture increases with higher flow rates and shorter column lengths.

The values in Table 2 were determined by estimating the humidity ratio of the ambient air with Eq. 23 and multiplying it by the product of the mass flow rate, and the time to saturation. The time to saturation was taken from the graph as the point where the dewpoint sharply rises.

These results provide practical information on how effectively the molecular sieve will dry air as air flows through it. Isotherms were also available but were of limited usefulness because they were determined using stationary air. Though these

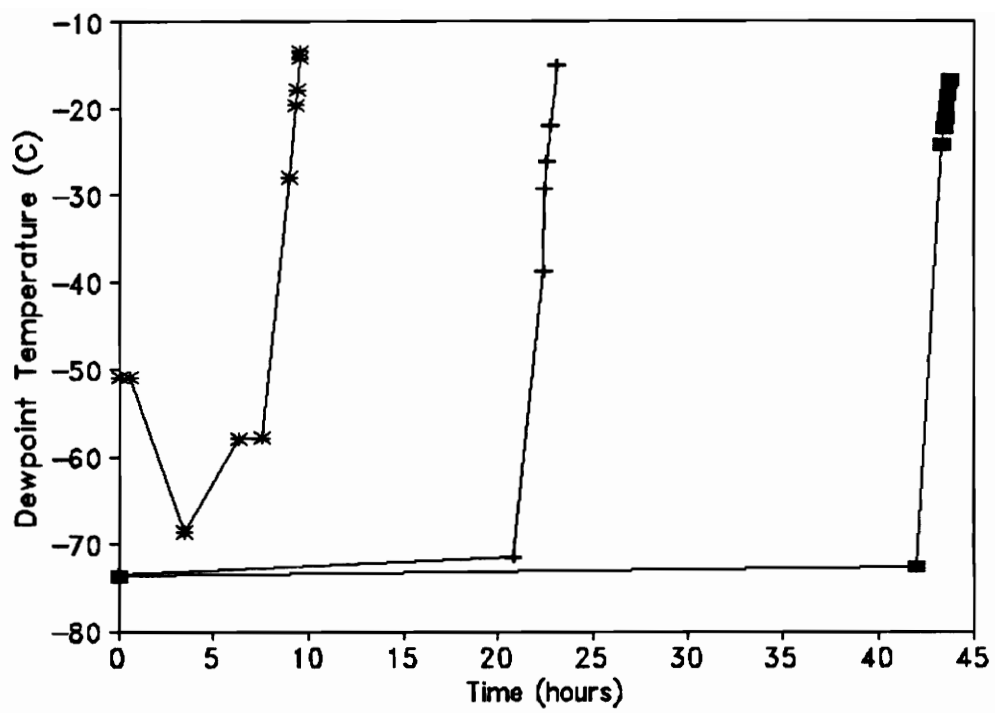


Fig. 35 Dewpoint temperature vs time for an air velocity of 0.037 m/s.

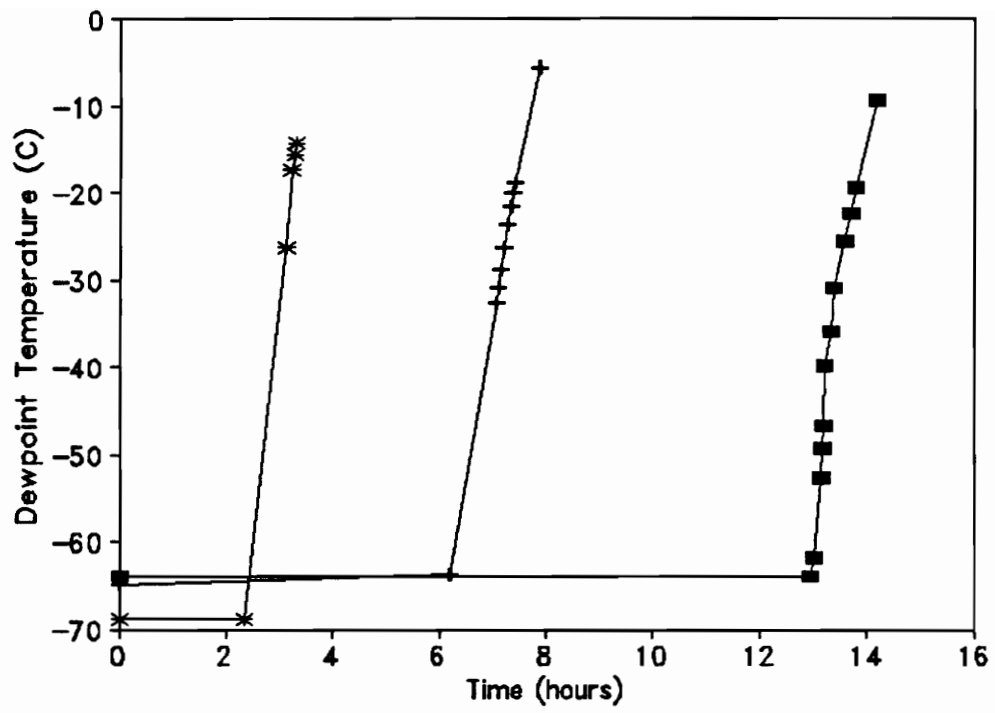


Fig. 36 Dewpoint temperature vs time for an air velocity of 0.11 m/s.

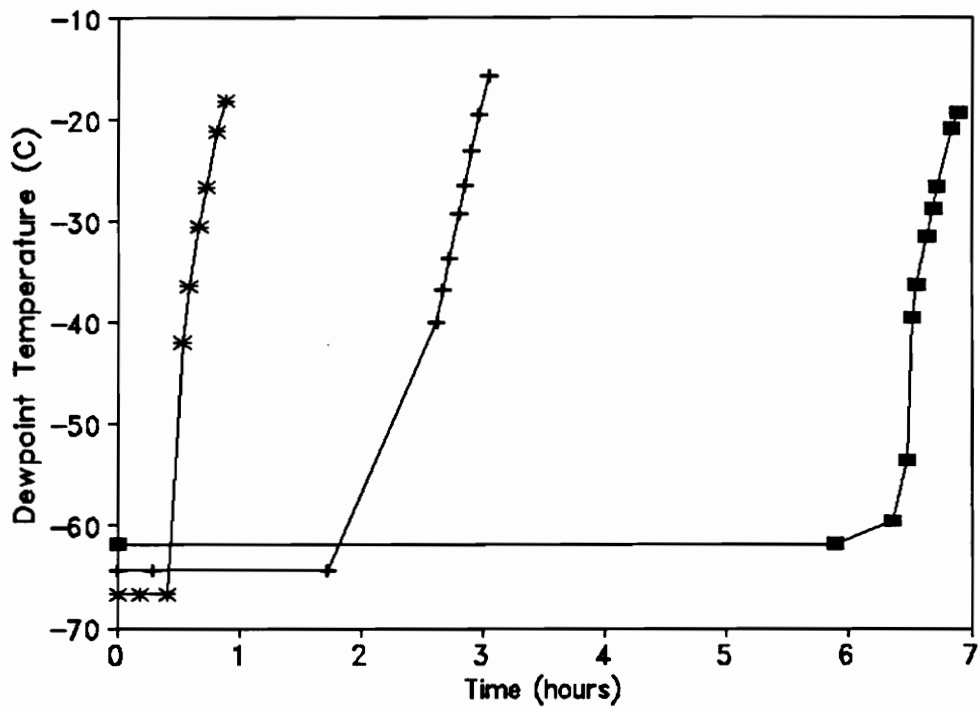


Fig. 37 Dewpoint temperature vs time for an air velocity of 0.22 m/s.

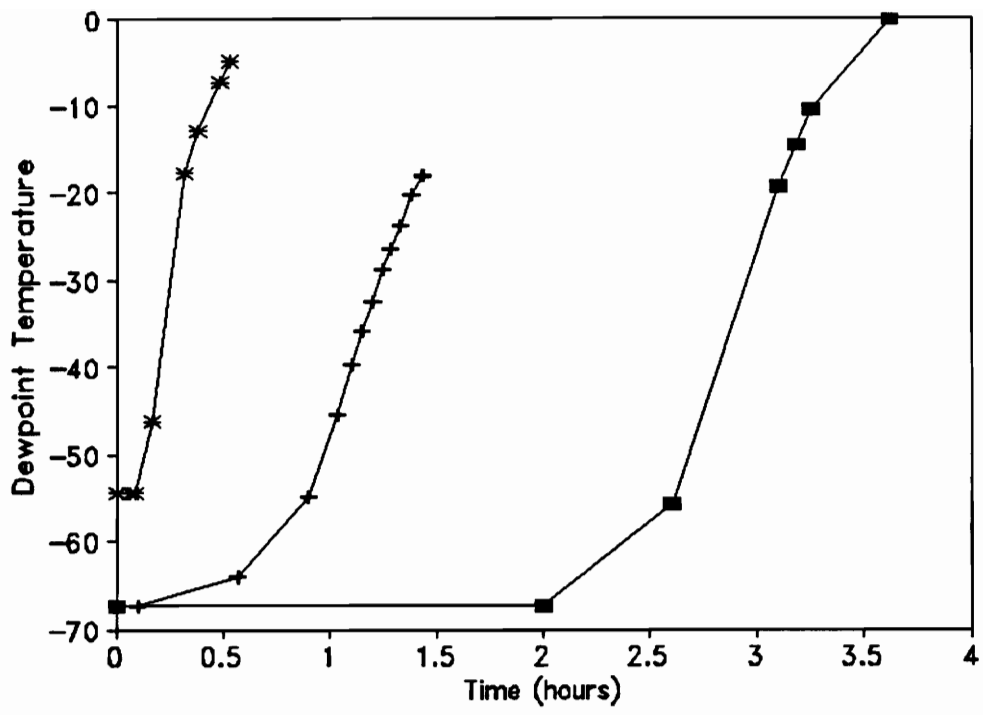


Fig. 38 Dewpoint temperature vs time for an air velocity of .44 m/s.

Table 2: Mass of desiccant necessary to absorb 1 g of moisture for air with a 12°C dewpoint and a 22°C temperature.

Column Length	Velocity			
	0.037 m/s g_d/g_w	0.11 m/s g_d/g_w	0.22 m/s g_d/g_w	0.44 m/s g_d/g_w
0.14 m	12	14	38	75.2
0.28 m	8.8	10	18	30
0.56 m	8.6	9	10	15

results do not necessarily allow direct correlation to any particular chamber temperature, chamber relative humidity, and moisture transfer rate, they were useful as a starting point in designing the desiccant column.

Appendix 3 Heat Transfer Model

Beginning with the heat transfer relation for a heat exchanger

$$q = UA\Delta T \quad (29)$$

and separating the heat transfer into heat transfer through the sample and heat transfer through the chamber wall gives

$$q = (UA)_c (T_a - T_{c1}) + (UA)_{spec} (T_{c2} - T_{c1}) \quad (30)$$

Considering that

$$R = \frac{1}{UA} \quad (31)$$

and referring to Fig. 39

$$R_{spec} = R_1 + R_2 + R_3 \quad (32)$$

and

$$R_c = \frac{1}{\frac{1}{R_3 + R_4 + R_5 + R_8} + \frac{1}{R_3 + R_7 + R_6 + R_8}} \quad (33)$$

The resistance terms are

$$R_1 = \frac{1}{h_1 A_2}$$

$$R_5 = \frac{\Delta x_5}{k_5 A_4}$$

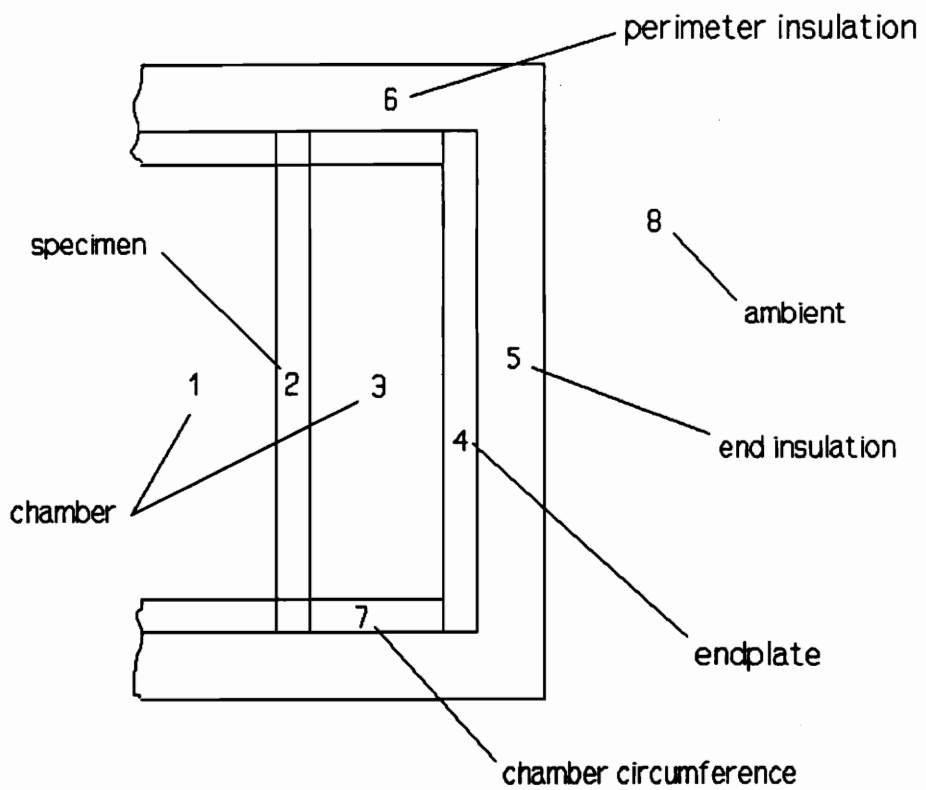


Fig. 39 Illustration of chamber thermal resistances.

$$R_2 = \frac{\Delta x_2}{k_2 A_2}$$

$$R_6 = \frac{\ln\left(\frac{r_{o6}}{r_{i6}}\right)}{2\pi k_6 L_6}$$

$$R_3 = \frac{1}{h_3 A_3}$$

$$R_7 = \frac{\ln\left(\frac{r_{o7}}{r_{i7}}\right)}{2\pi k_7 L_7}$$

$$R_4 = \frac{\Delta x_4}{k_4 A_4}$$

$$R_8 = \frac{1}{h_8 A_4}$$

Where the subscripts i and o represent inside and outside the chamber respectively.

The overall heat transfer coefficient for each section will be

$$UA_c = \frac{1}{R_{spec}} + S \quad (34)$$

and

$$UA_{spec} = \frac{1}{R_{spec}} + S \quad (35)$$

The shape factor accounts for two dimensional heat transfer effects at the corner and between the chambers. For the chamber the shape factor is

$$S = .54 \pi D k_{insulation} \quad (36)$$

Vita

The author, Robert Prentiss Crimm, was born in Newton, Mississippi on July 31, 1963. His childhood years were spent in Meridian, Mississippi. He graduated from Brigham Young University with a Bachelor of Science in Mechanical Engineering in December 1989. He entered Virginia Polytechnic Institute and State University in August 1990. He is a member of the American Society of Mechanical Engineers (ASME) and the Association of Energy Engineers (AEE). His future plans include moving to central Alabama to accept a position with International Paper, Inc. as a Project Engineer at the Hammermill Riverdale Mill in Selma, Alabama.